Journal for ImmunoTherapy of Cancer

Senescent cancer cell vaccines induce cytotoxic T cell responses targeting primary tumors and disseminated tumor cells

Yue Liu ,[1] Joanna Pagacz,[1] Donald J Wolfgeher,[1] Kenneth D Bromerg,[2] Jacob V Gorman,[2] Stephen J Kron[1]

To cite: Liu Y, Pagacz J, Wolfgeher DJ, *et al*. Senescent cancer cell vaccines induce cytotoxic T cell responses targeting primary tumors and disseminated tumor cells. *Journal for ImmunoTherapy of Cancer* 2023;**11**:e005862. doi:10.1136/jitc-2022-005862

► Additional supplemental material is published online only. To view, please visit the journal online (http://dx.doi.org/10.1136/jitc-2022-005862).

YL and JP contributed equally.

Accepted 31 January 2023

[1]Department of Molecular Genetics and Cell Biology and Committee on Cancer Biology, The University of Chicago, Chicago, Illinois, USA
[2]Oncology Discovery, AbbVie, North Chicago, Illinois, USA

Correspondence to
Dr Stephen J Kron;
skron@uchicago.edu

ABSTRACT

Background Immune tolerance contributes to resistance to conventional cancer therapies such as radiation. Radiotherapy induces immunogenic cell death, releasing a burst of tumor antigens, but this appears insufficient to stimulate an effective antitumor immune response. Radiation also increases infiltration of cytotoxic T lymphocytes (CTLs), but their effector function is short lived. Although CTL exhaustion may be at fault, combining immune checkpoint blockade with radiation is insufficient to restore CTL function in most patients. An alternative model is that antigen presentation is the limiting factor, suggesting a defect in dendritic cell (DC) function.

Methods Building on our prior work showing that cancer cells treated with radiation in the presence of the poly(ADP-ribose) polymerase-1 inhibitor veliparib undergo immunogenic senescence, we reexamined senescent cells (SnCs) as preventative or therapeutic cancer vaccines. SnCs formed in vitro were cocultured with splenocytes and evaluated by scRNA-seq to examine immunogenicity. Immature bone-marrow-derived DCs cocultured with SnCs were examined for maturation and activation by flow cytometry and T cell proliferation assays. Viable SnCs or SnC-activated DCs were injected subcutaneously, and vaccine effects were evaluated by analysis of immune response, prevention of tumor engraftment, regression of established tumors and/or potentiation of immunotherapy or radiotherapy.

Results Murine CT26 colon carcinoma or 4T1 mammary carcinoma cells treated with radiation and veliparib form SnCs that promote DC maturation and activation in vitro, leading to efficient, STING-dependent CTL priming. Injecting mice with SnCs induces antigen-specific CTLs and confers protection from tumor engraftment. Injecting immunogenic SnCs into tumor-bearing mice increases inflammation with activated CTLs, suppresses tumor growth, potentiates checkpoint blockade, enhances radiotherapy and blocks colonization by disseminated tumor cells. Addressing the concern that reinjecting tumor cells into patients may be impractical, DCs activated with SnCs in vitro were similarly effective to SnCs in suppressing established tumors and blocking metastases.

Conclusions Therapeutic vaccines based on senescent tumor cells and/or SnC-activated DCs have the potential to improve genotoxic and immune therapies and limit recurrence or metastasis.

WHAT IS ALREADY KNOWN ON THIS TOPIC

⇒ Although therapy-induced senescence is considered deleterious and implicated in therapy resistance, cancer recurrence and metastasis, there is also evidence that senescent cells (SnCs) can drive antitumor immunity.

WHAT THIS STUDY ADDS

⇒ Our study shows that dendritic cells (DCs) cocultured with SnCs become mature and activated and efficiently prime T cells through a STING-dependent mechanism. Injecting SnCs into mice induces antitumor immunity and serves as a cancer vaccine that potentiates immunotherapy and radiotherapy and suppresses growth of disseminated tumor cells. Injecting DCs activated by SnCs in vitro recapitulates SnC vaccine effects, confirming the mechanism.

HOW THIS STUDY MIGHT AFFECT RESEARCH, PRACTICE OR POLICY

⇒ Our observation that SnC-activated DCs can enhance therapy response and block metastatic spread in preclinical models points the way to personalized cancer vaccines formed by loading DCs with senescent patient tumor cells that will promote tumor regression and suppress distant spread.

BACKGROUND

Cellular senescence, where cells remain viable but irreversibly arrested as an outcome of cellular stress, serves critical roles in diverse physiological and pathological processes, including development, healing, aging and cancer.[1 2] Senescence is considered an important barrier to malignancy insofar as replicative senescence induced by telomere erosion can prevent unlimited proliferation while oncogene-induced senescence resulting from oncogenic or tumor suppressor mutations can block transformation. Although cancer cells are often considered immortal, they can undergo stress-induced senescence in response to genotoxic or other therapies,[3]

which may have both beneficial and deleterious effects on outcomes. Given these many links to malignancy, senescence is now considered a hallmark of cancer[4] and a potential target for cancer therapies.[5]

Senescent cells (SnCs) typically form when proliferating cells fail to complete cell division due to a persistent DNA damage checkpoint and/or mitotic catastrophe. As these SnCs form over a few days, they may undergo endoreduplication and continue to grow, often increasing dramatically in cell size. SnCs may remain viable indefinitely, persisting until they undergo cell death or are eliminated by immune surveillance. Reflecting persistent cell stress, SnCs typically display altered metabolism and gene expression, present distinct cell surface proteins and display an altered secretome, the senescence-associated secretory phenotype (SASP), characterized by expression of inflammatory mediators.[6]

The SASP, like SnCs themselves, has been considered a double-edged sword in modulating immune responses.[7] An immune-suppressive SASP has been reported to increase immune suppressing myeloid cells and inhibit antitumor T cell and NK cell responses. These effects may contribute to progression, resistance and recurrence, arguing for SnC elimination after therapy.[8] However, the immune surveillance mechanism that limits SnC accumulation has long been considered a critical mechanism in limiting age and stress-related disorders and carcinogenesis.[9] Oncogene-induced senescence facilitates the immune surveillance of premalignant cells by promoting the recruitment and activation of innate and adaptive immune cells, including monocytes, macrophages, neutrophils, NK cells and T cells.[10–12] This raises the question whether senescent cancer cells might retain the ability to drive antitumor immune response even after the onset of malignancy. Indeed, previous studies from our group and others have indicated that therapy-induced senescence is capable of promoting antitumor immunity and improving treatment outcomes.[13–15] For instance, SnCs formed in situ with ionizing radiation (IR) and poly(ADP-ribose) polymerase (PARP) inhibitor veliparib[13] or CDK4/6 inhibition[14] led to T cell-dependent antitumor immunity. Additionally, aneuploidy-associated senescence could promote NK cell-mediated tumor clearance.[15] Although features of the SASP might be primary determinants of immune response, cell surface expression of major histocompatibility complex (MHC) molecules and altered antigen presentation in SnCs may also play critical roles.[14]

Here, we revisited the immunogenic potential of senescent tumor cells in the form of a cancer vaccine. Single-cell RNA sequencing (scRNA-seq) analysis of splenocytes cocultured with SnCs suggested that DCs may be particularly responsive to and key mediators of SnC effects. Indeed, therapy-induced SnCs could promote DC activation and maturation via STING-dependent mechanisms and DCs activated by SnCs were effective at priming T cells. Consistent with our prior studies,[13] therapy-induced SnCs were effective as a preventative vaccine, inducing antigen-specific cytotoxic T cell responses and blocking engraftment of tumor cells. Examined as therapeutic vaccines, peritumoral injection of SnCs suppressed tumor growth on its own and increased the effectiveness of immune checkpoint blockade of programmed cell death ligand 1 (PD-L1) interaction with programmed cell death protein 1 (PD-1) in overcoming immunosuppression. Injecting SnCs combined with radiotherapy eliminated tumors. On their own, SnCs were able to suppress colonization by disseminated tumor cells (DTCs) in a breast cancer metastasis model. Importantly, injecting SnC-activated DCs rather than SnCs recapitulated these effects, serving as effective therapeutic vaccines to limit tumor growth and prevent colonization by DTCs. Translated to the clinic, adjuvant therapy with autologous or allogeneic DC vaccines activated with SnCs formed from transiently cultured patient tumor tissue may have significant value in enhancing local and systemic therapy to limit metastatic spread or recurrence.

MATERIALS AND METHODS

Cell lines and tissue culture

BALB/c-derived colon carcinoma cell line CT26 (HTB-85) and mammary carcinoma cell line 4T1 were obtained from ATCC. The cells were tested for mycoplasma contamination and authenticated by a short tandem repeat profile (IDEXX BioResearch) prior to performing experiments.

Cells were maintained in RPMI 1640 (Thermo Fisher Scientific) supplemented with 10% FBS (Atlanta Biologicals) and 1% penicillin/streptomycin (Thermo Fisher Scientific). The basic murine immune cell culture medium was RPMI 1640 (Thermo Fisher Scientific) supplemented with 10% heat-inactivated FBS (Thermo Fisher Scientific), 1% penicillin/streptomycin (Thermo Fisher Scientific) and 50 µM β-mercaptoethanol. All experiments were performed within 3 to 10 passages after thawing cells. At least three replicates were performed in all in vitro experiments.

Preparation of mouse BMDCs

Bone marrow-derived dendritic cells (BMDCs) were differentiated as previously described.[16] Briefly, bone marrow was isolated from 7-week to 8-week BALB/c mice, maintained in basic immune cell culture medium supplemented with 1 ng/mL mouse recombinant GM-CSF (PeproTech) and 200 ng/mL mouse recombinant Flt-3 ligand (PeproTech) for 14–16 days, changing medium on days 6, 9 and 12.

Animal models

For animal experiments, 6-week to 8-week BALB/c wild-type (WT) mice were purchased from Harlan-Envigo. NOD SCID gamma (NSG) mice were maintained by breeding. All mice used for these studies were procured and maintained following guidelines approved by the Institutional Animal Care and Use Committee. Tumor

volume was measured using calipers every 2–3 days from day 7 after subcutaneous tumor cell inoculation. Mice that did not develop palpable tumors within 10 days after inoculation were excluded from the study. For preventative cancer vaccines, mice were randomized to receive SnC vaccines. For therapeutic cancer vaccines, mice were randomized after tumor cell inoculation. At least 5 mice per group were used in all in vivo experiments reported here.

Chemical probes

Veliparib was provided by AbbVie. Etoposide, GSK461364, ABT-263, DMXAA and C178 were purchased from Cayman Chemical.

Preparation of SnC vaccine and SnC-activated DC vaccine

1×10^6 CT26 cells or 4T1 cells were seeded into T175 flasks, then treated with IR+veliparib (12 Gy+20 µM). After 5 days, SnCs were trypsinized and washed in phosphate-buffered saline (PBS), then resuspended in cold PBS to a final concentration of 5×10^6 cells/mL. To form an SnC-activated DC vaccine, naive BMDCs were cocultured with SnCs for 10–12 hours. Non-adherent BMDCs were collected and washed in PBS, then resuspended in cold PBS to a final concentration of 5×10^6 cells/mL. One hundred microliters of SnCs or SnC-activated DCs were injected as a vaccine dose.

Quantification and statistical analysis

Statistical significance was determined using the paired Student's t-test or logrank test as indicated. Calculations were performed using Prism software (GraphPad) or Excel. $p\leq0.05$ was considered statistically significant.

SA-β-Gal, SASP characterization, single-cell RNA sequencing (scRNA-seq), BMDC activation, T cell cross-priming, in vitro cell proliferation, Western blotting, immunofluorescence, AH-1 dextramer staining, in vivo vaccination, TIL analysis, lung colonization and histology assays are described in the online supplemental methods.

RESULTS

SnCs stimulate immune responses in vitro

To model the interactions of senescent tumor cells with the tumor immune microenvironment, we cocultured SnCs with splenocytes in vitro. CT26 murine colon carcinoma cells were treated with the PARP1/2 inhibitor veliparib (20 µM) along with IR (12 Gy) to induce immunogenic senescence, as has been shown in other cell lines.[13] After 5 days, more than 90% of the surviving CT26 cells had developed an SA-β-Gal$^+$ senescent phenotype (online supplemental figure S1A). Then, the SnCs or proliferating controls were cocultured for 3 days with splenocytes from CT26 tumor-bearing mice and non-adherent cells were collected for single-cell RNA sequencing (scRNA-seq), serving as a cells-as-sensors assay (online supplemental figure S1B). Seurat integration analysis resolved 11 cell clusters, including multiple types of immune cells known to contribute to the anti-tumor immune response (figure 1A–B and online supplemental figure S1C,D). Reanalysis after excluding the non-immune cell population and B cells allowed resolution of additional immune cell types classified in 8 clusters (figure 1C,D). Splenocytes cocultured with SnCs displayed markedly increased fractions of type 1 conventional dendritic cells (cDC1) and CD8$^+$ T cells compared with controls (figure 1EF and online supplemental figure S1C,D). Analyzing composite gene expression in the cDC1 cell clusters revealed marked differences in differentially expressed genes (DEGs) (online supplemental figure S1E). Biological process (BG) gene ontology (GO) analysis of the cDC1 indicated that coculture with SnCs upregulated pathways such as stress response, cytokine response, T cell activation and antigen processing (figure 1G). GO analysis with other databases revealed complementary patterns, including upregulation of antigen processing and presentation and type I interferon (IFN) signals (online supplemental figure S1F,G). These results suggest that DCs may be particularly responsive to senescent tumor cells and thereby may mediate the effects of SnCs on immune response.

SnCs promote DC activation and T cell priming in vitro

Our scRNA-seq studies encouraged us to further examine DCs to determine if SnCs might serve as a source of antigen for presentation. Considering that diverse stresses can induce cancer cell senescence, we investigated whether different senescence inducers might influence interactions with DCs. CT26 cells treated with IR (12 Gy), IR+veliparib (12 Gy+20 µM), topoisomerase II poison etoposide (2 µM) or PLK1 inhibitor GSK461364 (5 µM) displayed~65%, 90%, 95% and 95% SA-β-Gal$^+$ SnCs, respectively, at 5 days (figure 2A). Cells treated with dimethyl sulfoxide (DMSO) or veliparib alone were used as non-senescent controls. Compared with proliferating cells, SnCs secreted higher levels of cytokines and chemokines, including those that promote DC maturation/activation, such as CCL5 (online supplemental figure S2A,B). BMDCs were formed as described[16] by culturing BALB/c bone marrow in GM-CSF and Flt-3 ligand. To examine phagocytosis and/or trogocytosis, senescent or control cells were labeled with lipophilic dye PHK26 or the pH-sensitive fluorescent probe pHrodo Red and incubated with BMDCs for 6 hours. Transfer of PHK26 to DCs or uptake of pHrodo Red into DC endosomes or lysosomes were analyzed by flow cytometry (online supplemental figure S3A,B). Overall, SnCs were engulfed or nibbled more than proliferating cells and different senescence inducers appeared to influence uptake (figure 2B,C and online supplemental figure S4A). In turn, SnCs induced BMDC activation and maturation based on flow cytometric analysis of costimulatory molecules CD86 and CD80 and MHC I molecule H-2K^d (figure 2D and online supplemental figure S3C). SnCs also upregulated surface expression of PD-L1 on BMDCs (figure 2D). Similar experiments using BALB/c-derived

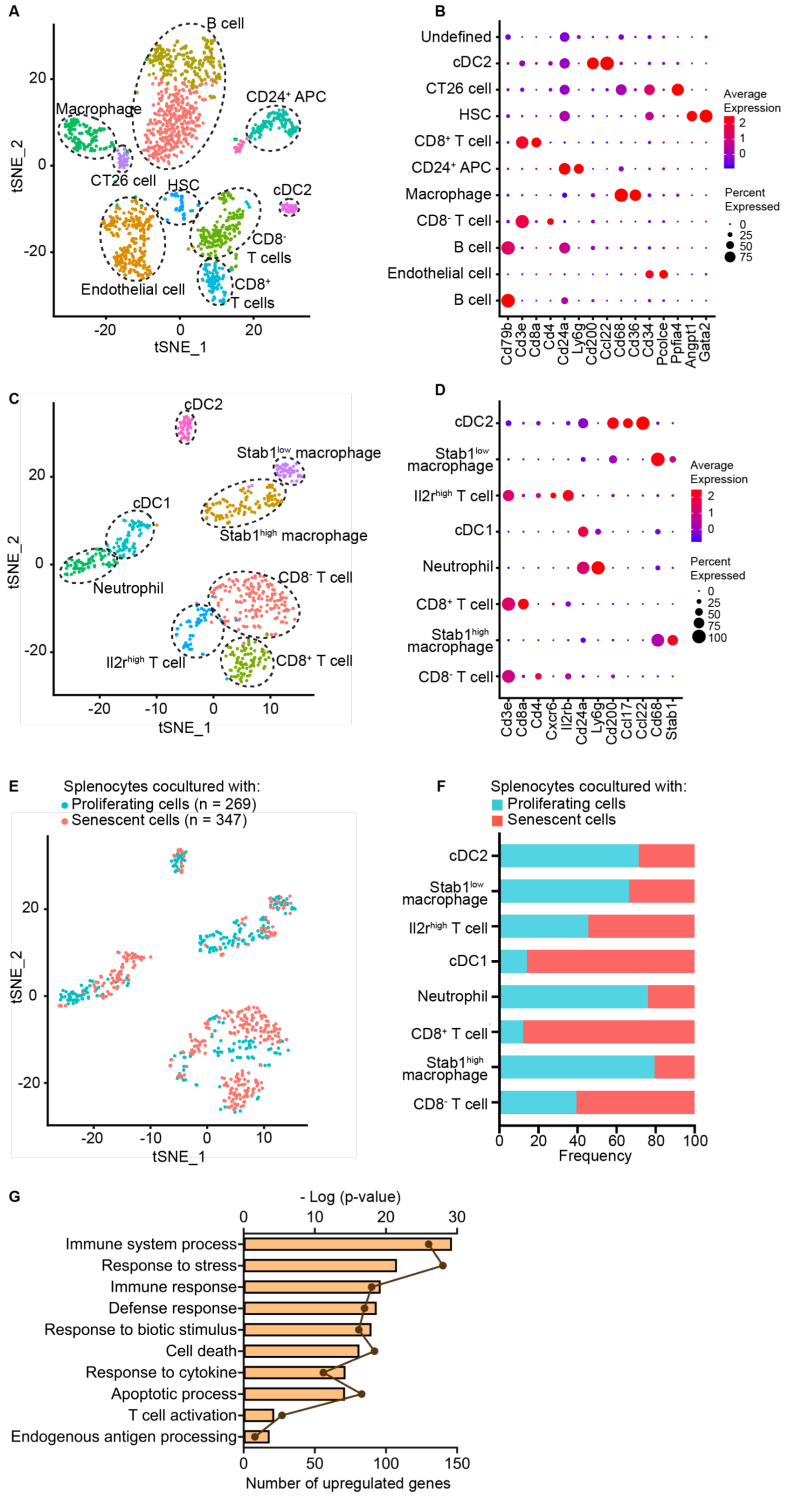

Figure 1 scRNA-seq cells-as-sensors assay reveals dendritic cell activation by SnCs. After coculture with CT26 SnCs or proliferating cells, splenocytes were analyzed by scRNA-seq, and the two datasets were pooled, yielding, (A) tSNE plot demonstrating 11 cell clusters from 1618 cells assigned to immune subsets as inferred from (B) dot plot indicating relative expression of marker genes in each cell cluster. (C–F) Reanalysis of pooled data after excluding cells from B cell, HSC, endothelial cell, CT26 and undefined clusters. (C) tSNE plot demonstrating 8 cell clusters from 616 cells with subsets inferred from (D) dot plot indicating relative expression of marker genes in each cell cluster. (E) tSNE plot indicating relative distributions of splenocytes cocultured with SnCs or proliferating cells. (F) Stacked bar graph indicating the relative frequency of splenocytes cocultured with SnCs or proliferating cells in each cluster, indicating enrichment of cDC1 and CD8$^+$ T cells. (G) Biological process gene ontology analysis of differential expressed genes (DEGs) among cDC1s. Shown are enriched, upregulated signaling pathways in the cDC1 population of splenocytes cocultured with SnCs vs proliferating cells. Dots indicate the number of DEGs and bars indicate the -Log10 (p value) for each enriched pathway. APC, antigen-presenting cell; cDC1, conventional type 1 dendritic cell; cDC2, conventional type 2 dendritic cell; HSC, hematopoietic stem cell; SnCs, senescent cells.

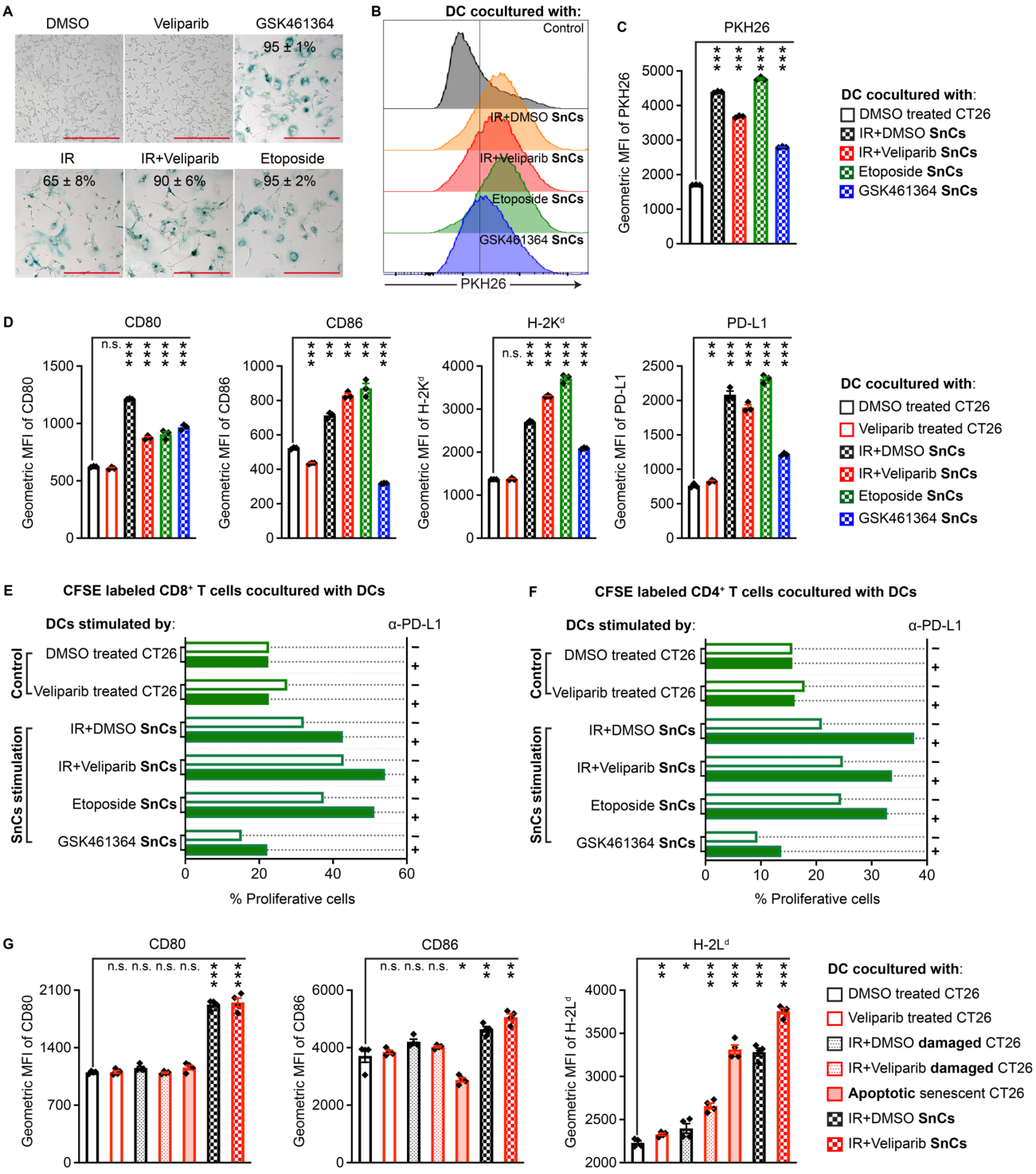

Figure 2 Senescent CT26 cells promote DC maturation/activation and CD8$^+$ T cell priming in vitro. (A) Compared with CT26 cells treated with DMSO vehicle or veliparib as controls, GSK461364, IR, IR+veliparib and etoposide each induced senescence after 5 days. Indicated is mean±SD of % SA-β-Gal-positive cells from five fields. Scale bars: 200 µm. (B) Representative histograms indicating effective uptake of PHK26-labeled SnCs by BMDCs. (C) Geometric mean fluorescence intensity (MFI) bar graph demonstrating uptake from each cell population (n=3, mean±SD). Paired t-test. (D) CT26 SnCs and controls prepared as in (A) were cocultured with BMDCs overnight, followed by flow cytometry analysis for CD80, CD86, MHC I and PD-L1 maturation and activation markers. Shown are bar graphs of geometric MFI for the viable CD11c$^+$/CD103$^+$ DC population (n=3, mean±SD). Paired t-test. (E and F) Analysis of T cell priming by SnC-activated DCs. Shown are the % proliferative (CFSE-diluted) fraction of viable CD8$^+$/CD4$^-$ (E) or CD8$^-$/CD4$^+$ (F) T cells. (G) Comparison of BMDC activation by CT26 proliferating cells, damaged cells, apoptotic SnCs or live SnCs. Shown are bar graphs of geometric MFI (n=4, mean±SD). Paired t-test. For statistical analysis, ***p<0.001, **0.001<p<0.01, *0.01<p<0.05, n.s. p>0.05. BMDCs, bone marrow-derived dendritic cells; CFSE. carboxyfluorescein succinimidyl ester; DC, dendritic cell; DMSO, dimethyl sulfoxide; IR, irradiation; PD-L1, programmed cell death ligand 1; SnCs, senescent cells.

4T1 murine mammary carcinoma cancer cells revealed that 4T1 SnCs induced similar responses in BMDCs (online supplemental figures S4B and S5A–C).

To examine DC antigen presentation induced by SnCs, we stimulated BMDCs with SnCs or control CT26 cells and then incubated the BMDCs with carboxyfluorescein succinimidyl ester (CFSE) -labeled splenocytes collected from BALB/c mice immunized with irradiated CT26 cells. CFSE dilution was examined after 5 days by flow cytometry (online supplemental figure S3D). BMDCs cocultured with non-senescent, control CT26 cells, treated with veliparib or not, induced less than 27% of proliferating $CD8^+$ T cells. DCs cocultured with SnCs induced by IR, IR+veliparib, etoposide or GSK461364 stimulated 32.1%, 42.9%, 37.5% and 15%, respectively, of proliferating $CD8^+$ T cells (figure 2E and online supplemental figure S6A). After coculture with CT26 SnCs, except those induced by GSK461364, BMDCs also increased the proliferation of $CD4^+$ T cells (figure 2F and online supplemental figure S6C). Potentially reflecting the induction of PD-L1 on BMDCs cocultured with SnCs, T cells displayed a higher proliferation rate in the presence of α-PD-L1 antibody to block PD-1 signaling (figure 2E,F and online supplemental figures S6A–D). Similar results were observed with 4T1 cells (online supplemental figures S7A–D). Interestingly, both conditioned media and cell lysate from SnCs could stimulate DCs, although with distinct patterns (online supplemental figure S8A).

While SnCs can promote a DC-mediated T cell response, their immunogenicity appears to depend on the conditions of senescence induction, raising the question whether SnCs display distinct immunogenicity from other forms of damaged cells, viable or not.[17] To examine viability, we treated CT26 SnCs with the senolytic Bcl-2 inhibitor ABT263, which resulted in 51% Annexin V^+/PI^+ and 44% Annexin V^+/PI^- apoptotic SnCs (online supplemental figure S3E). Alternatively, CT26 cells were treated with IR±veliparib but cocultured with BMDC after 1 day, prior to adopting a senescent phenotype, rather than after 5 days as before. Thus, BMDCs were cocultured with live senescent, apoptotic senescent, damaged or proliferating CT26 cells, followed by flow cytometric analysis of the surface expression levels of CD80, CD86 and another MHC I molecule H-$2L^d$. The results indicated that live SnCs are most effective at stimulating DC maturation and activation (figure 2G).

STING signaling is required for senescence-mediated DC activation

Therapy-induced SnCs displayed nuclear DNA double-strand breaks and cytoplasmic DNA accumulation, resulting in the activation of cGAS/STING/TBK/IRF3 signaling and the production of type I IFNs (online supplemental figures S8B–E). It has long been considered that the STING signaling axis plays a critical role in antitumor immunity.[18] Recent work has demonstrated that activated STING and IRF3 are required for $CD8^+$ T cell priming in response to tumor antigens.[19] To examine the effects of STING activation on the immunogenicity of therapy-induced SnCs, we generated a population of STING knockout (KO) CT26 cells using CRISPR/Cas9/gRNA RNP to target the STING ORF (online supplemental figure S9A). Electroporation with a scrambled gRNA was used as control. After passaging the cells, cellular senescence was induced by IR, IR+veliparib, etoposide or GSK461364. Although STING KO did not affect cell proliferation, senescence induction, γH2AX foci persistence or cytoplasmic DNA accumulation (online supplemental figures S9B–F), it decreased MHC I surface expression and CCL5 secretion in SnCs (online supplemental figures S10A–C). Notably, the ability of CT26 SnCs with STING KO to stimulate the maturation and activation of BMDCs was also diminished (figure 3). Similarly, we pretreated SnCs formed from CT26 or 4T1 cells and proliferating controls with 4 µM covalent STING inhibitor C178. As with the STING KO SnCs, STING inhibition decreased the ability of SnCs to induce BMDC maturation and activation (online supplemental figures S11A–C and S12A–C), indicating that STING signaling in SnCs mediates DC activation.

To explore whether STING activation alone is sufficient to explain the immunogenicity, we treated proliferating CT26 cells for 2 days with DMXAA, a STING agonist. Despite showing robust activation of TBK1, the DMXAA-treated proliferating CT26 cells appeared unable to activate DCs (online supplemental figure S13A,B). Additionally, the DC activation ability of SnCs, whether STING WT or KO, was not affected by DMXAA (online supplemental figure S13B). These results indicate that STING signaling may be necessary, but not sufficient, for SnCs to display immunogenicity.

SnCs induce antigen-specific anti-tumor immune response in vivo

SnCs formed with IR+veliparib appeared to be particularly effective at activating DCs to prime T cells in vitro. To evaluate the immune response to these SnCs in vivo, we injected BALB/c mice subcutaneously (SQ) with 0.5×10^6 senescent CT26 cells or PBS. Injection of SnCs did not result in tumor growth. However, compared with controls, mice inoculated with SnCs on the dorsum displayed swollen inguinal draining lymph nodes (DLNs) 2 days after injection (figure 4A). CT26 is a BALB/c-derived tumor that expresses the endogenous MuLV retroviral envelope glycoprotein 70 (gp70) and presents the MHC I H-$2L^d$-restricted immunodominant peptide SPSYVYHQF (AH1, residues 423–431).[20] Flow cytometric analysis confirmed a significant increase in AH1-specific $CD8^+$ T cells in the DLNs after SnC injection (figure 4B,C).

Considering that AH1-specific CTLs are sufficient to eliminate CT26 tumors,[20] we examined SnCs as a preventative vaccine. To test protection against tumor engraftment, BALB/c mice were left untreated or inoculated with CT26 SnCs and then, after 5 days, injected with 0.5×10^6 proliferating CT26 cells (figure 4D). While control BALB/c mice developed tumors that grew to the humane

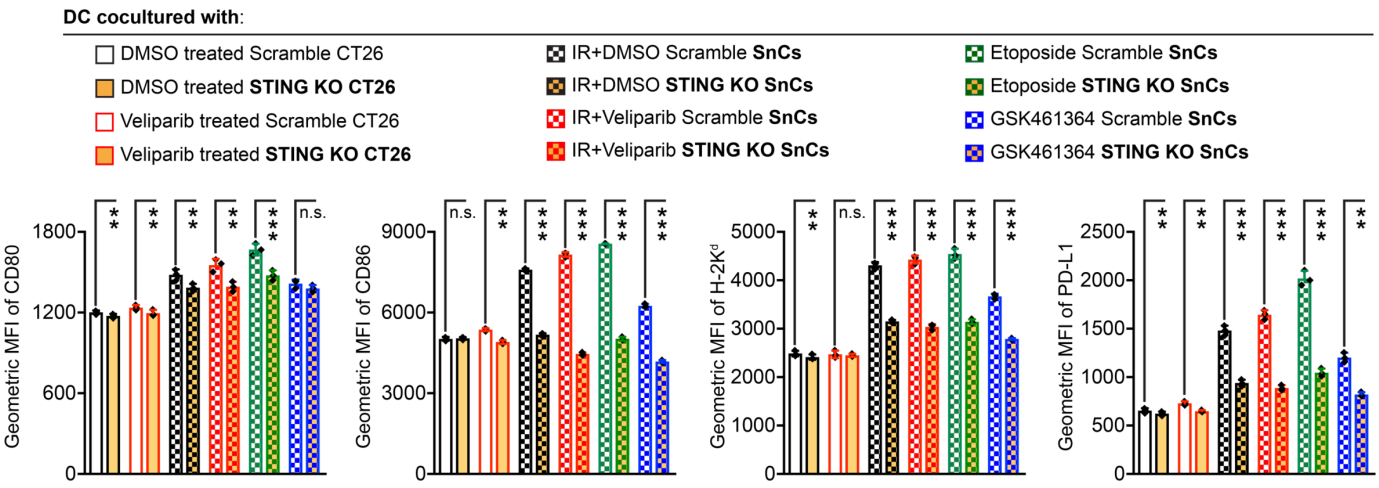

Figure 3 STING signaling mediates SnC activation of BMDCs. For analysis of DC activation/maturation, Cas9 STING KO and scramble control CT26 cells were treated with DMSO, veliparib, IR (12 Gy), IR+veliparib (12 Gy+20 µM), etoposide (2 µM) or GSK461364 (5 µM) for 5 days, followed by coculturing with BMDCs overnight. Then, the viable $CD11c^+/CD103^+$ DC population was analyzed for expression of CD80, CD86, H-$2K^d$ and PD-L1. Shown are bar graphs of geometric MFI (n=3, mean±SD). Paired t-test. ***p<0.001, **0.001<p<0.01, *0.01<p<0.05, n.s. p>0.05. BMDCs, bone marrow-derived dendritic cells; DC, dendritic cell; DMSO, dimethyl sulfoxide; MFI, mean fluorescence intensity; IR, irradiation; KO, knock out; PD-L1, programmed cell death ligand 1; SnCs, senescent cells.

endpoint within 4 weeks, no tumors formed in mice that had been treated with SnCs (figure 4E). Notably, STING KO SnCs were less effective at preventing tumor engraftment in BALB/c mice (online supplemental figure S13C). SnC injection did not affect tumor formation or growth in immunodeficient NSG BALB/c mice (figure 4F). Consistent with the shared expression of gp70,[21] injection of CT26 SnCs also displayed modest suppression of tumor formation after SQ injection of 0.5×10^6 proliferating 4T1 cells. While anti-PD-L1 antibody (α-PD-L1) offered no protection on its own, treatment with CT26 SnCs and then α-PD-L1 significantly increased protection against engraftment of 4T1 cells (figure 4G,H). Overall, these results suggest that SnCs formed with IR+veliparib with intact STING signals display significant immunogenicity in vivo.

SnC vaccines slow tumor growth and potentiate therapy

To have broad practical value, tumor cell-derived vaccines must display benefits in treating established tumors. To evaluate SnCs as a therapeutic vaccine, BALB/c mice bearing subcutaneous CT26 tumors were treated with two peritumoral injections of 0.5×10^6 CT26 SnCs twice in a 5-day interval with or without a single intravenous (IV) injection of α-PD-L1 in between. Considering that the immune profile changes according to tumor size,[22] we initiated treatment either on day 9 (average tumor volume ~60 mm^3) (figure 5A and online supplemental S14A) or day 12 (average tumor volume ~150 mm^3) (online supplemental figure S15A) after tumor inoculation. For treatment beginning on day 9, SnCs and α-PD-L1 treatment each suppressed tumor growth, while the SnCs+α-PD-L1 combination resulted in complete regression of three of six tumors (figure 5B,C and online supplemental figures S14B–E). We observed a similar pattern with 4T1 tumors when treatment was initiated on day 9 using a 4T1 SnC vaccine and/or α-PD-L1, with both SnCs and SnCs+α-PD-L1 leading to tumor elimination (online supplemental figures S16A–G). When treatment of CT26 tumors was initiated on day 12, α-PD-L1 had little effect on its own, but SnCs slowed tumor growth appreciably and the combination treatment displayed moderate tumor control, though no tumor elimination (online supplemental figures S15B–G).

As an alternative to α-PD-L1, we examined combining the SnC vaccine with radiation to treat established tumors. Here, we again formed subcutaneous CT26 tumors and treated them starting on day 9 or 12 with two peritumoral injections of 0.5×10^6 SnCs over a 5-day interval, with or without a single dose of 10 Gy irradiation (IR) in between. As before, SnCs alone suppressed tumor growth, but the effect was far greater on smaller tumors (figure 5D–F and online supplemental figures S15H–J). On its own, a single dose of 10 Gy IR significantly delayed tumor growth, but most tumors recovered and resumed growth within 10 days. However, combining SnCs with radiation significantly enhanced the effects of radiation, resulting in tumor elimination by 2 weeks post-treatment for both smaller and larger tumors (online supplemental figures S14F-J and S15K-N).

To investigate the effects of peritumoral injection of SnCs on the tumor microenvironment, we obtained tumors 5 days after treatment with SnCs, α-PD-L1, SnCs+α-PD-L1, IR or SnCs+IR, and used flow cytometry to evaluate total $CD45^+$ immune infiltrates, $CD11c^+/CD103^+$ DCs, $CD3^+/CD4^+$ helper T cells (T_h), $CD3^+/CD8^+$ cytotoxic T lymphocytes (CTLs) and $CD3^-/CD49b^+$ natural killer (NK) cells (online supplemental figures S3G–H). Compared with control, peritumoral injection of SnCs led

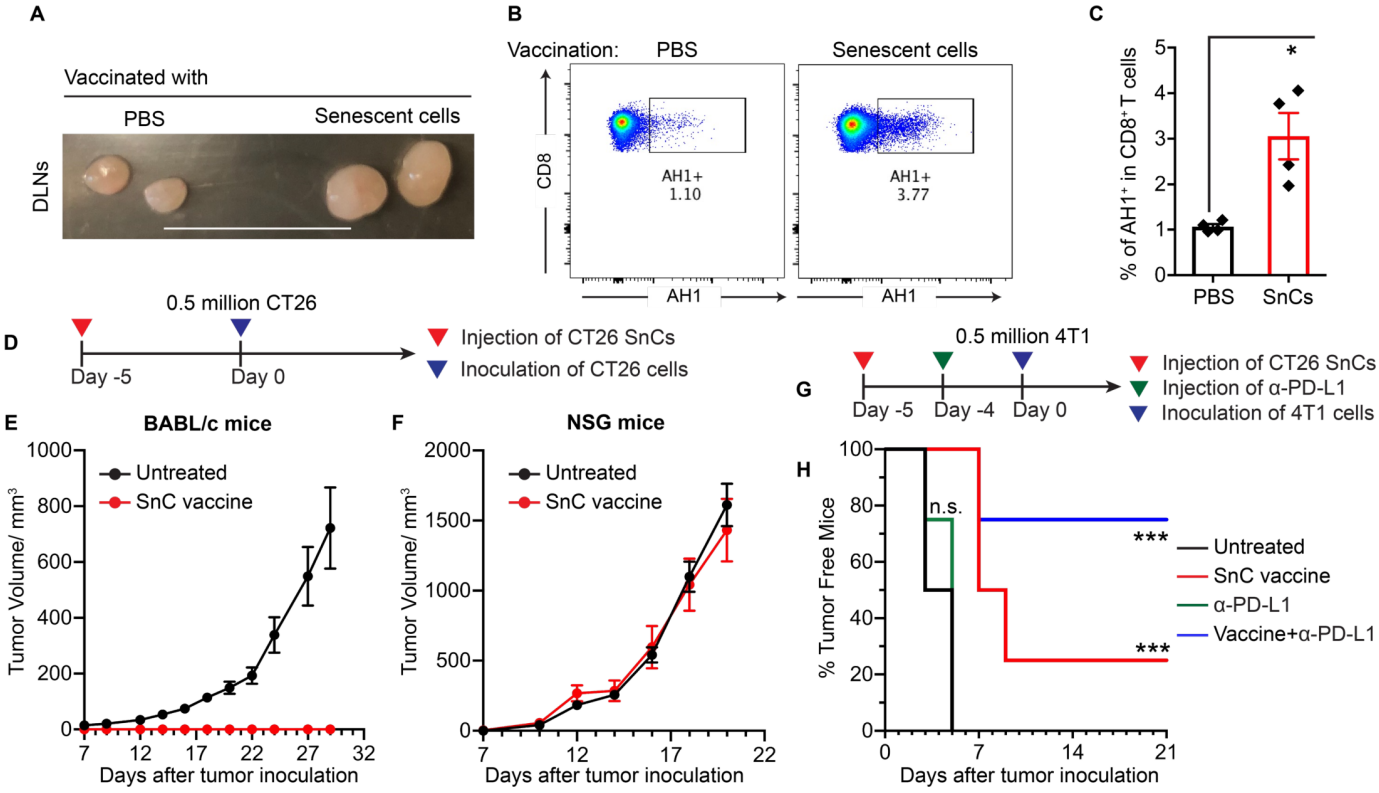

Figure 4 SnC vaccine induces tumor-specific CTLs and blocks tumor engraftment in immune-competent hosts. (A) Representative mouse inguinal draining lymph nodes (DLNs) collected from BALB/c mice 2 days after subcutaneous injection of 0.5×10^6 CT26 SnCs or PBS. Scale bar: 1 cm. (B and C) Dissociating DLNs for analysis by flow cytometry demonstrates increased $CD8^+$ T cell binding to H-$2L^d$ dextramer presenting AH1. (B) Representative 2D plots showing AH1-binding TCR^+ cells in gate. (C) Histogram of % AH1-binding TCR^+ cells. Shown by individual mice (dot) and mean±SD (bar). Paired t-test. (D) Experimental schema for CT26 SnC vaccination and CT26 cell challenge in vivo. Growth kinetics of tumors in BALB/c (E) or immunodeficient NSG mice (F) after receiving SnCs on day −5 followed by challenge with 0.5×10^6 CT26 proliferating cells on day 0. Shown is tumor growth plotted as mean±SEM. (G) Experimental schema for CT26 SnC vaccination and 4T1 cell challenge, with or without α-PD-L1. BALB/c mice injected with 0.5×10^6 CT26 SnCs at day −5, α-PD-L1 at day −4 or both treatments were challenged with 0.5×10^6 4T1 proliferating cells on day 0 and examined for palpable tumors at 2-day to 3-day intervals. (H) Kaplan-Meier analysis of 4T1 tumor incidence over time. Logrank test. ***p<0.001, **0.001<p<0.01, *0.01<p<0.05, n.s. p>0.05. CTLs, cytotoxic T lymphocytes; NSG, NOD SCID gamma; PBS, phosphate-buffered saline; PD-L1, programmed cell death ligand 1; SnCs, senescent cells.

to a significant increase in tumor-infiltrating lymphocytes (TILs), and this effect was amplified by both α-PD-L1 and 10 Gy (figure 5G). Similarly, immunofluorescence analysis of tumor sections demonstrated increased levels of activated CTLs ($CD8^+$/$Perforin^+$ or $CD8^+$/$Granzyme\ B^+$) after SnC vaccine, whether alone or in combination with α-PD-L1 or 10 Gy (figure 5H and online supplemental figure S17A,B). A similar pattern of enhanced immune response was observed in 4T1 tumors treated with 4T1 SnCs alone or in combination with α-PD-L1 (online supplemental figures S18A–D).

SnC vaccines suppress lung colonization after tail vein injection of tumor cells

While conventional therapies may be sufficient to eradicate primary tumors, distant spread via metastasis lacks effective treatments. Used in the adjuvant setting, immunotherapies including tumor cell vaccines offer the potential to eliminate DTCs and micrometastases and thereby suppress distant recurrence.[23] Toward modeling the spread of breast cancer from primary tumors to the lungs, we injected 6×10^4 proliferating 4T1 cells via the tail vein to colonize the lungs of BALB/c mice (day 0). Tail vein injection appears to offer a faster and simpler model to form lung metastases with similar biology to those produced by orthotopic tumors that spread via spontaneous metastasis.[24] To examine preventative or therapeutic vaccination, 0.5×10^6 4T1 SnCs were injected subcutaneously into mice on days −5 and −1 or on days 1 and 5, respectively (figure 6A). To examine the effects of SnC vaccine on DTCs and resulting metastases, we collected the lungs on day 21 for microscopic and histological examination. While the untreated mice developed an average of 17 metastatic nodules on the lung surface, the preventative SnC vaccine protected three out of five mice from developing any visible metastatic nodules and the therapeutic SnC vaccine reduced lung surface metastases to an average of four (figure 6B). Histological analysis of lung sections confirmed that the SnC vaccine displayed

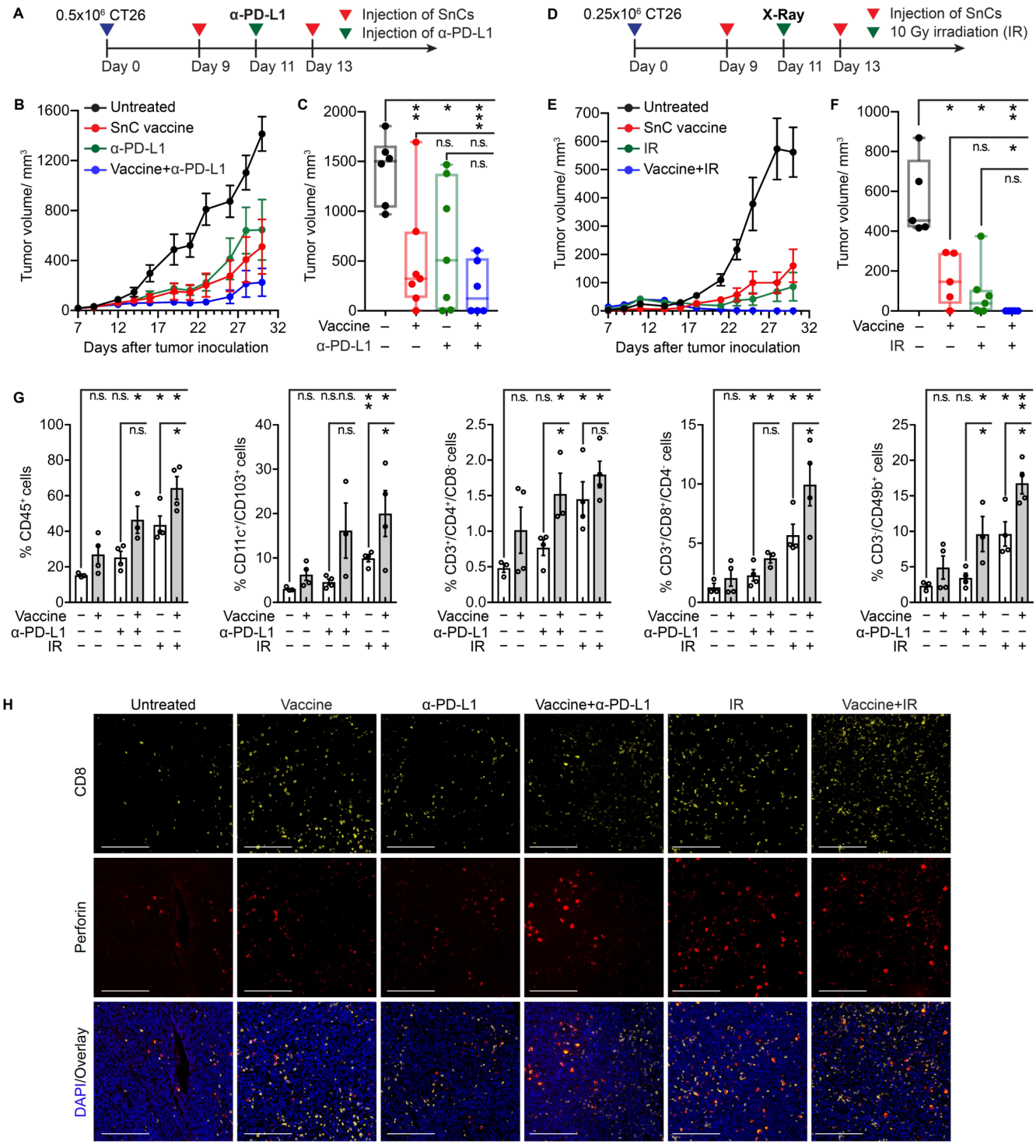

Figure 5 SnC vaccines suppress tumor growth, potentiate cancer therapies and promote tumor immune infiltrates. (A–C) SnC vaccine enhances checkpoint blockade. (A) Experimental schema for treating CT26 tumor-bearing mice with vaccine and/or α-PD-L1. (B) Growth kinetics of CT26 tumors untreated, treated with SnC vaccine, α-PD-L1 or combination therapy (mean±SEM). (C) CT26 tumor size at day 30. Shown by individual tumor (dot) and size range (box and whisker). Paired t-test. (D–F) SnC vaccine potentiates radiotherapy. (D) Experimental schema for treating CT26 tumor-bearing mice with vaccine and/or irradiation (IR). (E) Growth kinetics of CT26 tumors untreated, treated with SnC vaccine, IR or combination therapy (mean±SEM). (F) CT26 tumor size at day 30. Shown by individual tumor (dot) and size range (box and whisker). Paired t-test. (G) Analysis of immune infiltrate in CT26 tumors treated as in (A) and (D) reveals increased CTLs and NK cells after SnC vaccine+IR. Analyzing the viable (Zombie Yellow$^-$) single cell population, total immune, DC, T_h, CTL and NK cell were quantified. Shown by individual tumor (open circle) and mean±SD (bar). Paired t-test. (H) Detection of activated CTL infiltrate in situ in CT26 tumors confirms SnC vaccine effects. The tumors examined in (G) were evaluated by immunofluorescence staining for CD8 (yellow), perforin (red) and DAPI (blue). Scale bars: 200 µm. For statistical analysis, ***p<0.001, **0.001<p<0.01, *0.01<p<0.05, n.s. p>0.05. CTLs, cytotoxic T lymphocytes; DC, dendritic cell; NK, natural killer; PD-L1, programmed cell death ligand 1; SnCs, senescent cells.

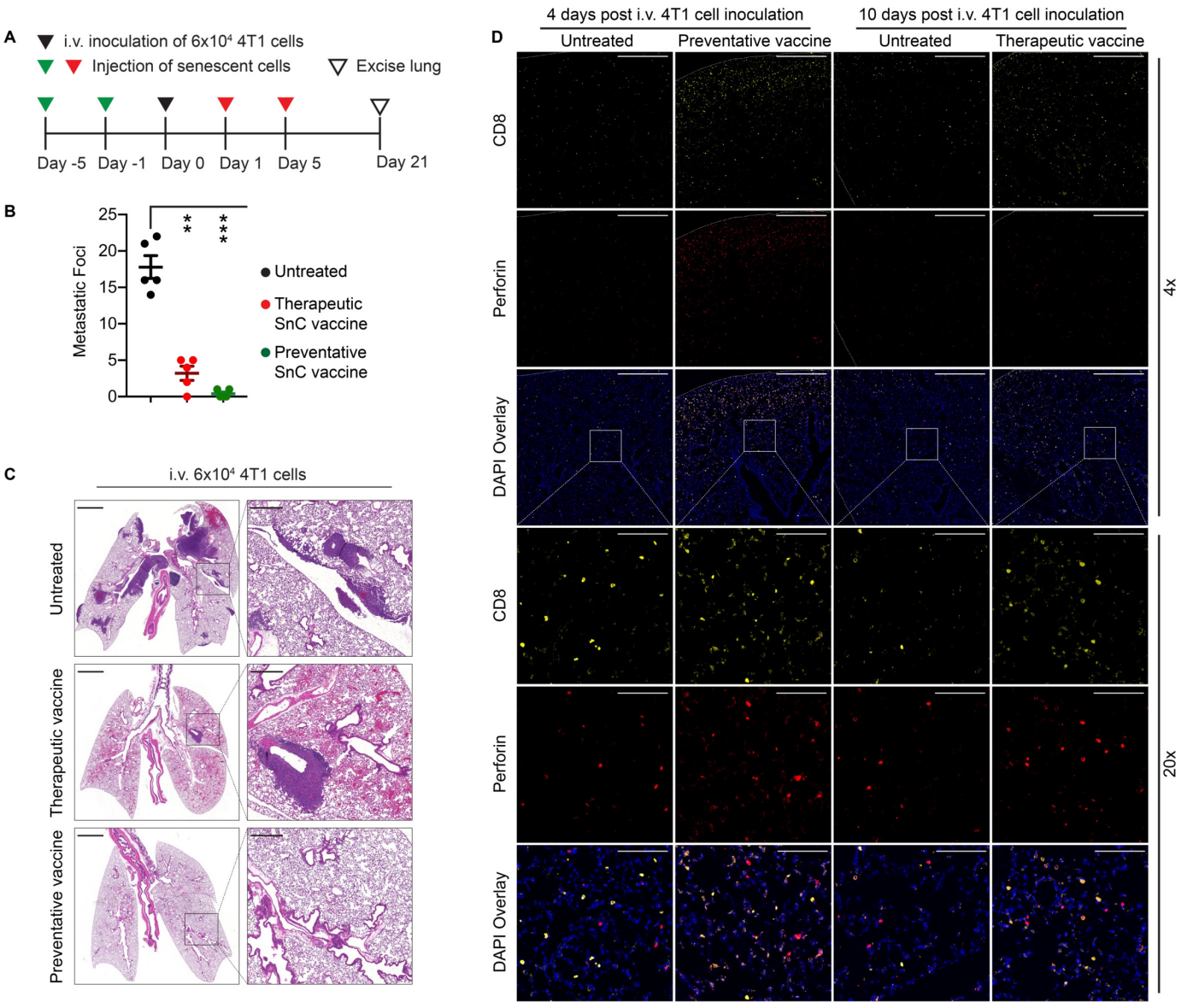

Figure 6 SnC vaccines suppress 4T1 lung colonization by disseminated tumor cells. (A) Experimental schema for testing SnC vaccines against 4T1 lung colonization; 6×10^4 proliferating 4T1 cells were inoculated through tail vein (i.v.) into BALB/c mice on day 0, delivering disseminated tumor cells and lungs collected at day 21 to examine colony formation. To examine SnCs as preventative or therapeutic vaccine, 0.5×10^6 senescent 4T1 cells were injected subcutaneously on days −5 and −1 or days 1 and 5, respectively. (B) Effects of SnC vaccines on lung surface metastatic foci. Shown are counts from individual animals (dot), with mean±SEM (bar). Paired t-test. ***p<0.001, **0.001<p<0.01. (C) Representative H&E staining demonstrating tumor colonization in lung parenchyma, vessels and/or airways at low magnification with inset zoomed to high magnification. Scale bars: 2 mm (left) and 50 µm (right). (D) Immunofluorescence analysis of the lung CTL infiltrates at 5 days after SnC injection, staining for CD8 (yellow), perforin (red) and DAPI (blue) under 4x or 20x magnification. Scale bars: 500 µm (4x) and 100 µm (20x). CTL, cytotoxic T lymphocyte; SnCs, senescent cells.

a similar protective effect against metastases formed in the lung parenchyma (figure 6C). Similar protection was observed for IV injection of 8×10^4 proliferating cells, which otherwise produced significantly higher numbers of metastatic foci (online supplemental figurea S19A–C). Immunofluorescence analysis of lungs, whether collected on day 4 (4 days after 4T1 cell inoculation and 5 days after preventative SnC vaccine) or on day 10 (10 days after 4T1 cell inoculation and 5 days after therapeutic SnC vaccine) revealed a similar increase in activated CTLs ($CD8^+$/$perforin^+$) in pulmonary tissue (figure 6D).

SnC-activated DC vaccine recapitulates the effects of SnC vaccine and induces antitumor memory responses

While the vaccine-like effects of SnCs may reflect multiple mechanisms, our in vitro and in vivo results suggest a model where the injected SnCs are taken up by DCs to induce maturation and activation, leading to expansion of tumor-responsive CTLs in the DLNs. Thus, we examined whether peritumoral injection of ex vivo activated DCs could recapitulate the therapeutic vaccine effects of injected SnCs. To prepare the DC vaccine, the BMDCs were cocultured with IR+veliparib-induced CT26 SnCs

for ~12 hours. The resulting activated, antigen-loaded DCs were then injected adjacent to CT26 tumors, twice over 5 days starting on day 12, with or without a single X-ray dose of 10 Gy in between (figure 7A). SnC-activated DCs caused only modest tumor growth inhibition on their own but the combination with IR led to the elimination of most tumors (figure 7B,C and online supplemental figurea S20A–E). To test immunological memory, mice whose tumors had been eliminated by the SnC-activated DCs+IR treatment were re-challenged with 0.5×10^6 proliferating CT26 cells (figure 7D). No tumor development was observed over 3 weeks in the treated mice versus 100% tumor take within 1 week in naive mice (figure 7E).

To confirm systemic effects, we investigated whether SnC-activated DCs could suppress 4T1 lung metastasis. BALB/c mice were injected IV with 6×10^4 4T1 cells on day 0 and then DCs were injected SQ on days 1 and 5, with or without IV α-PD-L1 on day 3 (figure 7F). Examining the lungs on day 21, α-PD-L1 had no effect on its own while the SnC-activated DCs significantly reduced the development of lung metastases, with or without α-PD-L1 (figure 7G,H). Histology analysis revealed a similar pattern, where the SnC-activated DCs markedly suppressed tumor formation in the lung parenchyma, with or without α-PD-L1 (figure 7I).

DISCUSSION

While the first observation of tumor elimination in mice after vaccination with irradiated tumor tissue was made over a century ago[25] and studies showing enhanced radiation response after injection of irradiated tumor tissue were published over five decades ago both in rodents[26] and in patients with breast cancer,[27] irradiated autologous tumor cell-based vaccines have yet to enter clinical practice. The dramatic success of immune checkpoint blockade immunotherapy has revived interest in cancer vaccines, which might provide a complementary means to help eliminate primary and distant tumors and then maintain durable surveillance against recurrence.[28 29] Most recent efforts to increase immunogenicity of lethally irradiated tumor cell vaccines have relied on engineering the cells to express GM-CSF or other cytokines toward promoting antigen uptake and presentation, with several examples under clinical investigation such as GVAX for pancreatic and prostate cancers[30] and Vigil for ovarian cancer.[31] Among many alternative strategies to produce immunogenic whole tumor cell vaccines, preclinical studies have reported encouraging results with early ferroptotic cells,[32] necroptotic cells[33] and etoposide-injured cells.[34] Senescent tumor cells have multiple attractive features as cancer vaccines insofar as SnCs can no longer proliferate but persist indefinitely, offering the potential for prolonged release of cancer antigens and immune-stimulating cytokines.[13 35] Here, we have reexamined injecting SnCs as preventative and therapeutic vaccines, finding them effective in limiting tumor formation and growth, sensitizing tumors to immunotherapy and radiation, and inhibiting tumor metastasis. Further, we find that injecting SnC-activated DCs recapitulates the effects of SnCs, providing a realistic path to the clinic.

Immune checkpoint blockade immunotherapy directed at maintaining CTL activity in the face of immunosuppressive signals in the tumor microenvironment such as PD-L1 has impacted the treatment and outcomes for many cancers, but overall response rates remain close to 25%, similar to adverse event rates.[36] Resistance to checkpoint blockade may be as simple as a lack of tumor-reactive CTLs to reactivate or protect, suggesting a need for complementary approaches to enhance tumor antigen presentation. Conventional cancer therapies including radiation can be effective triggers for immunogenic cell stress and cell death (ICD),[17] providing both antigen and adjuvant to serve as a vaccine in situ that may help drive antitumor immune responses. In particular, ICD can encourage DCs to collect tumor antigens and carry them into secondary lymphoid organs for antigen presentation, leading to antigen-specific T cell responses.[29] Although originally linked to cells succumbing to genotoxic stress as by necrosis, the definition of ICD has broadened to include diverse forms of cell death such as necroptosis, ferroptosis and parthanatos. Nonetheless, radiation-induced ICD on its own does not appear to be sufficient to overcome immunosuppression or to dramatically improve the response to checkpoint blockade.

Cellular senescence occurs when cellular damage is irreversible but not sufficient to force outright cell death.[17 37] Accordingly, immunogenic senescence and ICD share multiple driving mechanisms, including persistent DNA damage signaling, mitochondrial dysfunction, oxidative damage and deregulated autophagy. The resulting stress signaling may enhance immunogenicity by changing cell surface ligands, factors released from the cells and/or contents of exosomes or other vesicles. In both senescence and ICD, the increased antigenicity can be at least partially ascribed to the upregulation of MHC class I-dependent antigen-presenting machinery. Additionally, both senescence and ICD provide potent adjuvant signals through display or release of damage-associated molecular patterns (DAMPs) and secretion of numerous bioactive factors, including cytokines, chemokines and metabolic intermediates. While release of adjuvant factors from ICD can either be active or passive due to the change of membrane permeability and/or integrity, it is usually considered an active process in SnCs via the SASP. Along with some differences, ICD and senescence share specific features that influence immunogenicity, including but not limited to release of type I IFNs and the alarmin HMGB1.[37]

Much like immunosuppressive DAMPs, SASP factors can recruit myeloid-derived suppressor cells or have other effects that limit the cytotoxicity of NK cells and $CD8^+$ T cells.[38 39] Other dark sides of the SASP include paracrine signals that may promote tumor cell survival and dormancy. As such, therapy-induced senescence may play a detrimental role in the tumor microenvironment,

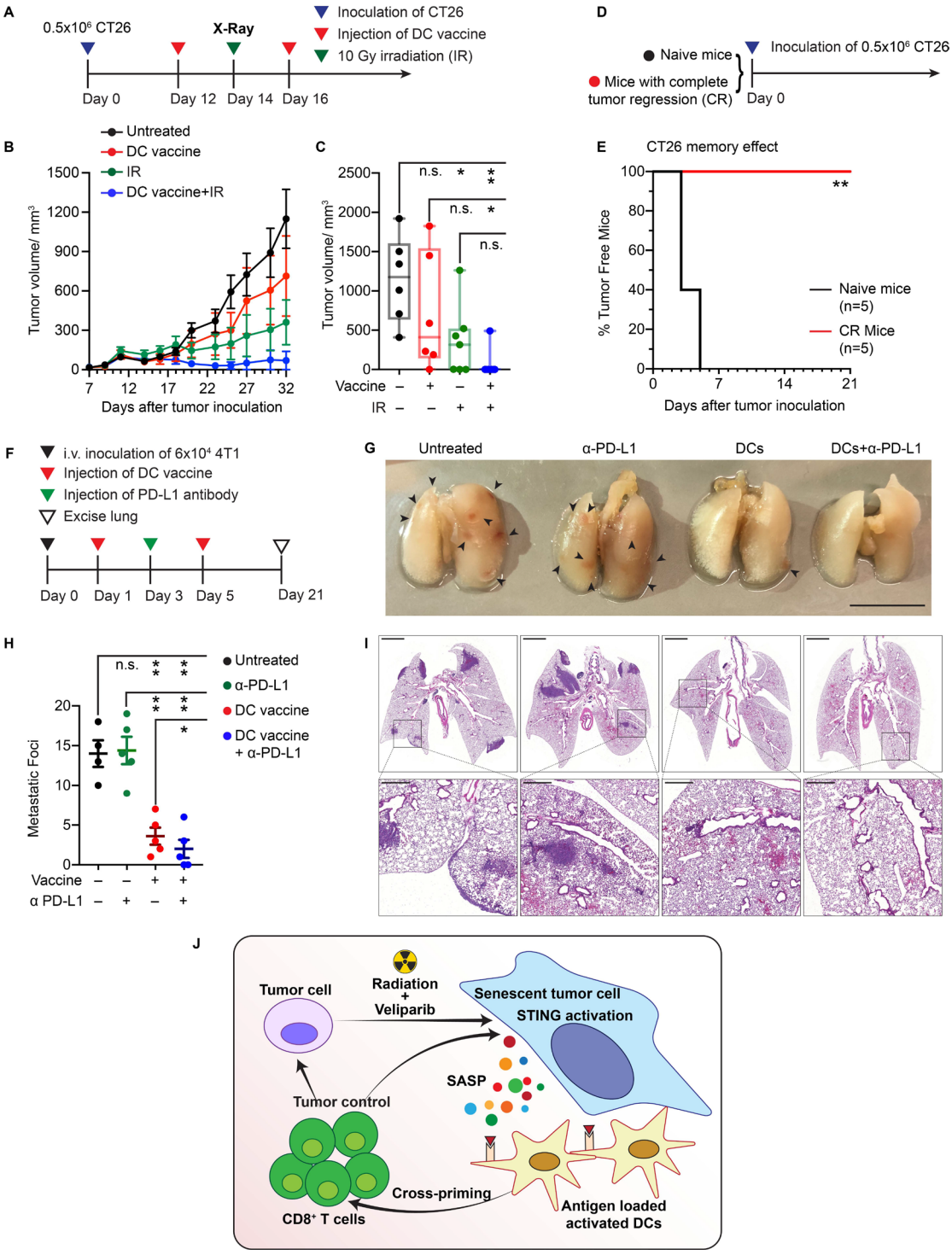

Figure 7 SnC-activated DC vaccine potentiates radiotherapy and suppresses lung colonization. (A) Experimental schema for treating CT26 tumor-bearing mice with SnC-activated DC vaccine and/or external beam irradiation. (B) Growth kinetics of CT26 tumors untreated, treated with vaccine, 10 Gy or combination therapy (mean±SEM). (C) CT26 tumor size at day 32 after tumor cell inoculation. Shown are individual tumor size (dot) and size range (box and whisker). Paired t-test. (D) Experimental schema for challenging naive mice or mice from the group received combination therapy and achieved a complete response. (E) Kaplan-Meier analysis of tumor development over time (n=5 per group). Logrank test. (F) Experimental schema for treating mice with SnC-activated DC vaccines to limit lung colonization. (G) Representative images of lungs from each treatment group. Scale bar: 1 cm. (H) Quantification of metastatic foci on lung surface. Shown are counts from individual lungs (dot), with mean±SEM (bar). Paired t-test. (I) Representative H&E staining of tumor colonization in lung parenchyma at low magnification with inset zoomed to high magnification. Scale bars: 2 mm (upper) and 50 µm (lower). For statistical analysis, ***p<0.001, **0.001<p<0.01, *0.01<p<0.05, n.s. p>0.05. (J) Model for how cellular damage and STING activation promotes immunogenicity of therapy-induced SnCs, leading to DC activation, stimulation of tumor antigen-reactive cytotoxic T cells and an effective adaptive immune response, eliminating surviving tumor cells. DC, dendritic cell; SnCs, senescent cells.

contributing to resistance and recurrence. In order to maximize tumor cell clearance without incurring adverse consequences, a one–two punch strategy for cancer therapy has been proposed,[8 40–42] where treatment with genotoxic cancer therapy that promotes therapy-induced senescence is followed by selective elimination of the senescent cancer cells. The second punch might be mediated by senolytic small molecules or immunotherapies.

Our results cannot answer the question whether senescent tumor cells are predominantly beneficial or detrimental. An attractive hypothesis is that when SnC formation is acute, beneficial effects and potential for immune clearance may be the greatest, while persistent SnCs mediate chronic, deleterious inflammation and other toxic effects.[43] An added benefit of greater SnC immunogenicity is that it may potentiate rapid immune clearance and limit SnC persistence, reducing the deleterious effects of the SASP in the tumor microenvironment. Taken together with this work, prior studies[13 35] along with exciting new results published while this paper was under consideration[44 45] provide strong evidence that SnCs can be immunogenic, inducing a cytotoxic T cell response with potential to not only clear SnCs but also prevent or eliminate tumors.

A critical pathway linked to the immunogenicity of radiation-induced ICD and senescence is STING signaling, resulting from cGAS binding to cytoplasmic DNA, activation of STING and TBK1, and increased expression of type I IFNs, cytokines and class I MHC, which facilitates immune response and recognition.[46] STING activation in tumors also promotes CTL infiltration. When STING was knocked out or inhibited, SnCs lost the ability to stimulate DCs, consistent with previously defined roles for STING in DC maturation and activation.[19] Although the specific mechanism remains to be studied, increased secretion of CCL5 and/or expression of MHC I may underlie STING-mediated immunogenicity in SnCs.

A concern that may prevent personalized SnC vaccines from reaching the clinic is the potential of reintroducing viable tumor cells that may contaminate the SnC preparation and/or arise due to escape from senescence.[47] Considering that SnCs efficiently activate DCs to prime T cells in vitro, we explored whether we could simply replace injecting SnCs with SnC-pulsed DCs. DC vaccines[48] are already practical with several preparations pulsed with peptide or protein antigens having advanced to the clinic, where most have displayed modest benefits. Vaccines based on autologous or allogeneic DCs fused or loaded with tumor cells or pulsed with lysates have also been studied. Recent interest has shifted to exploiting ICD to enhance tumor cell antigenicity and DC functionality.[49] Here, we have described a novel approach for activating and loading DCs by coculture with immunogenic senescent tumor cells in vitro. Subcutaneous vaccination with SnC-activated DCs elicits both local and systemic effects, leading to growth suppression of established tumors and DTCs. Injection of SnC-activated DCs enhanced the effects of anti-PD-L1 checkpoint blockade, and most mice treated with both radiation and SnC-activated DCs displayed tumor elimination and antitumor memory. Personalized therapies based on SnC-activated DCs may be both safe and practical. Loading by coculture with patient tumor-derived SnCs appears compatible with ongoing advances such as off-the-shelf DCs and other emerging strategies to improve DC production and function.[50] Overall, our results suggest the clinical potential to develop senescent tumor cells and SnC-activated DC vaccines for immunotherapy to enhance conventional therapy and prevent recurrence and metastasis.

Acknowledgements We thank Ani Solanki from the University of Chicago Animal Resource Center for assistance with tail vein injections, Elena Efimova for scientific advice and our colleagues at The University of Chicago and AbbVie for helpful support.

Contributors Conceptualization: YL, JP, SJK; methodology: YL, JP; visualization: YL, JP, DW; writing and editing: YL, JP, DW, KDB, JVG, SJK; funding acquisition: SJK; supervision: KDB, JVG, SJK; project administration and guarantor: SJK.

Funding These studies were supported by: AbbVie/UChicago collaboration award (SJK, KDB, JVG). METAvivor Translational Research Award (SJK). NIH R01 CA199663 (SJK). NIH R01 CA217182 (SJK). NIH R01 CA258737 (SJK). This work utilized service cores supported by: University of Chicago Comprehensive Cancer Center support grant NIH P30 CA014599.

Competing interests SJK is a co-founder of OncoSenescence. KDB and JVG are employees of AbbVie. The other authors declare that they have no competing interests.

Patient consent for publication Not applicable.

Ethics approval Not applicable.

Provenance and peer review Not commissioned; externally peer reviewed.

Data availability statement Data are available upon reasonable request. Further information and requests for resources and reagents should be directed to and will be fulfilled by Stephen Kron (skron@uchicago.edu).

ORCID iD

Yue Liu http://orcid.org/0000-0002-8344-9756

REFERENCES

1 Childs BG, Gluscevic M, Baker DJ, *et al*. Senescent cells: an emerging target for diseases of ageing. *Nat Rev Drug Discov* 2017;16:718–35.
2 Calcinotto A, Kohli J, Zagato E, *et al*. Cellular senescence: aging, cancer, and injury. *Physiol Rev* 2019;99:1047–78.
3 Lee S, Schmitt CA. The dynamic nature of senescence in cancer. *Nat Cell Biol* 2019;21:94–101.
4 Hanahan D. Hallmarks of cancer: new dimensions. *Cancer Discov* 2022;12:31–46.
5 Wang B, Kohli J, Demaria M. Senescent cells in cancer therapy: friends or foes? *Trends Cancer* 2020;6:838–57.

6 Basisty N, Kale A, Jeon OH, *et al*. A proteomic atlas of senescence-associated secretomes for aging biomarker development. *PLoS Biol* 2020;18:e3000599.
7 Faget DV, Ren QH, Stewart SA. Unmasking senescence: context-dependent effects of SASP in cancer. *Nat Rev Cancer* 2019;19:439–53.
8 Wang L, Lankhorst L, Bernards R. Exploiting senescence for the treatment of cancer. *Nat Rev Cancer* 2022;22:340–55.
9 Ovadya Y, Landsberger T, Leins H, *et al*. Impaired immune surveillance accelerates accumulation of senescent cells and aging. *Nat Commun* 2018;9:5435.
10 Kang T-W, Yevsa T, Woller N, *et al*. Senescence surveillance of pre-malignant hepatocytes limits liver cancer development. *Nature* 2011;479:547–51.
11 Iannello A, Thompson TW, Ardolino M, *et al*. P53-Dependent chemokine production by senescent tumor cells supports NKG2D-dependent tumor elimination by natural killer cells. *J Exp Med* 2013;210:2057–69.
12 Xue W, Zender L, Miething C, *et al*. Senescence and tumour clearance is triggered by p53 restoration in murine liver carcinomas. *Nature* 2007;445:656–60.
13 Meng Y, Efimova EV, Hamzeh KW, *et al*. Radiation-Inducible immunotherapy for cancer: senescent tumor cells as a cancer vaccine. *Mol Ther* 2012;20:1046–55.
14 Goel S, DeCristo MJ, Watt AC, *et al*. Cdk4/6 inhibition triggers anti-tumour immunity. *Nature* 2017;548:471–5.
15 Wang RW, Viganò S, Ben-David U, *et al*. Aneuploid senescent cells activate NF-κB to promote their immune clearance by NK cells. *EMBO Rep* 2021;22:e52032.
16 Mayer CT, Ghorbani P, Nandan A, *et al*. Selective and efficient generation of functional batf3-dependent CD103+ dendritic cells from mouse bone marrow. *Blood* 2014;124:3081–91.
17 Kroemer G, Galassi C, Zitvogel L, *et al*. Immunogenic cell stress and death. *Nat Immunol* 2022;23:487–500.
18 Yum S, Li M, Frankel AE, *et al*. Roles of the cgas-STING pathway in cancer immunosurveillance and immunotherapy. *Annu Rev Cancer Biol* 2019;3:323–44. 10.1146/annurev-cancerbio-030518-055636 Available: https://www.annualreviews.org/toc/cancerbio/3/1
19 Kwon J, Bakhoum SF. The cytosolic DNA-sensing cGAS-STING pathway in cancer. *Cancer Discov* 2020;10:26–39.
20 Huang AY, Gulden PH, Woods AS, *et al*. The immunodominant major histocompatibility complex class I-restricted antigen of a murine colon tumor derives from an endogenous retroviral gene product. *Proc Natl Acad Sci U S A* 1996;93:9730–5.
21 Yang D, Ud Din N, Browning DD, *et al*. Targeting lymphotoxin beta receptor with tumor-specific T lymphocytes for tumor regression. *Clin Cancer Res* 2007;13:5202–10.
22 Nesseler JP, Lee M-H, Nguyen C, *et al*. Tumor size matters-understanding concomitant tumor immunity in the context of hypofractionated radiotherapy with immunotherapy. *Cancers (Basel)* 2020;12:714.
23 Ganesh K, Massagué J. Targeting metastatic cancer. *Nat Med* 2021;27:34–44.
24 Rashid OM, Nagahashi M, Ramachandran S, *et al*. Is tail vein injection a relevant breast cancer lung metastasis model? *J Thorac Dis* 2013;5:385–92.
25 Contamin A. Immunisation contre le cancer de la souris inoculee avec des tumeurs modifiees par les rayons X. *Compt Rend Acad Sci* 1910;150:128–9.
26 HADDOW A, ALEXANDER P. An immunological method of increasing the sensitivity of primary sarcomas to local irradiation with X rays. *Lancet* 1964;1:452–7.
27 Anderson JM, Kelly F, Wood SE, *et al*. Stimulatory immunotherapy in mammary cancer. *Br J Surg* 1974;61:778–84.
28 Jou J, Harrington KJ, Zocca M-B, *et al*. The changing landscape of therapeutic cancer vaccines-novel platforms and neoantigen identification. *Clin Cancer Res* 2021;27:689–703.
29 Saxena M, van der Burg SH, Melief CJM, *et al*. Therapeutic cancer vaccines. *Nat Rev Cancer* 2021;21:360–78.
30 Soiffer RJ, Kooshesh KA, Ho V. Whole tumor cell vaccines engineered to secrete GM-CSF (GVAX). *ImmunoMedicine* 2021;1.
31 Rocconi RP, Stanbery L, Madeira da Silva L, *et al*. Long-Term follow-up of gemogenovatucel-T (vigil) survival and molecular signals of immune response in recurrent ovarian cancer. *Vaccines (Basel)* 2021;9:894.
32 Efimova I, Catanzaro E, Van der Meeren L, *et al*. Vaccination with early ferroptotic cancer cells induces efficient antitumor immunity. *J Immunother Cancer* 2020;8:e001369.
33 Aaes TL, Kaczmarek A, Delvaeye T, *et al*. Vaccination with necroptotic cancer cells induces efficient anti-tumor immunity. *Cell Rep* 2016;15:274–87.
34 Sriram G, Milling LE, Chen J-K, *et al*. The injury response to DNA damage in live tumor cells promotes antitumor immunity. *Sci Signal* 2021;14:705.
35 Hao X, Zhao B, Zhou W, *et al*. Sensitization of ovarian tumor to immune checkpoint blockade by boosting senescence-associated secretory phenotype. *IScience* 2021;24:102016.
36 Ribas A, Wolchok JD. Cancer immunotherapy using checkpoint blockade. *Science* 2018;359:1350–5.
37 Galluzzi L, Yamazaki T, Kroemer G. Linking cellular stress responses to systemic homeostasis. *Nat Rev Mol Cell Biol* 2018;19:731–45.
38 Faget DV, Ren Q, Stewart SA. Unmasking senescence: context-dependent effects of SASP in cancer. *Nat Rev Cancer* 2019;19:439–53.
39 Takasugi M, Yoshida Y, Hara E, *et al*. The role of cellular senescence and SASP in tumour microenvironment. *FEBS J* 2, 2022.
40 Zhang JW, Zhang D, Yu BP. Senescent cells in cancer therapy: why and how to remove them. *Cancer Lett* 2021;520:68–79.
41 Fletcher-Sananikone E, Kanji S, Tomimatsu N, *et al*. Elimination of radiation-induced senescence in the brain tumor microenvironment attenuates glioblastoma recurrence. *Cancer Res* 2021;81:5935–47.
42 Fitsiou E, Soto-Gamez A, Demaria M. Biological functions of therapy-induced senescence in cancer. *Semin Cancer Biol* 2022;81:5–13.
43 van Deursen JM. The role of senescent cells in ageing. *Nature* 2014;509:439–46.
44 Chen H-A, Ho Y-J, Mezzadra R, *et al*. Senescence rewires microenvironment sensing to facilitate antitumor immunity. *Cancer Discov* 2023;13:432–53.
45 Marin I, Boix O, Garcia-Garijo A, *et al*. Cellular senescence is immunogenic and promotes antitumor immunity. *Cancer Discov* 2023;13:410–31.
46 Hopfner KP, Hornung V. Molecular mechanisms and cellular functions of cGAS-STING signalling. *Nat Rev Mol Cell Biol* 2020;21:501–21.
47 Saleh T, Bloukh S, Carpenter VJ, *et al*. Therapy-induced senescence: an “old” friend becomes the enemy. *Cancers (Basel)* 2020;12:822.
48 Saxena M, Bhardwaj N. Re-emergence of dendritic cell vaccines for cancer treatment. *Trends Cancer* 2018;4:119–37.
49 Lamberti MJ, Nigro A, Mentucci FM, *et al*. Dendritic cells and immunogenic cancer cell death: a combination for improving antitumor immunity. *Pharmaceutics* 2020;12:256.
50 Saxena M, Balan S, Roudko V, *et al*. Towards superior dendritic-cell vaccines for cancer therapy. *Nat Biomed Eng* 2018;2:341–6.

Figure S1

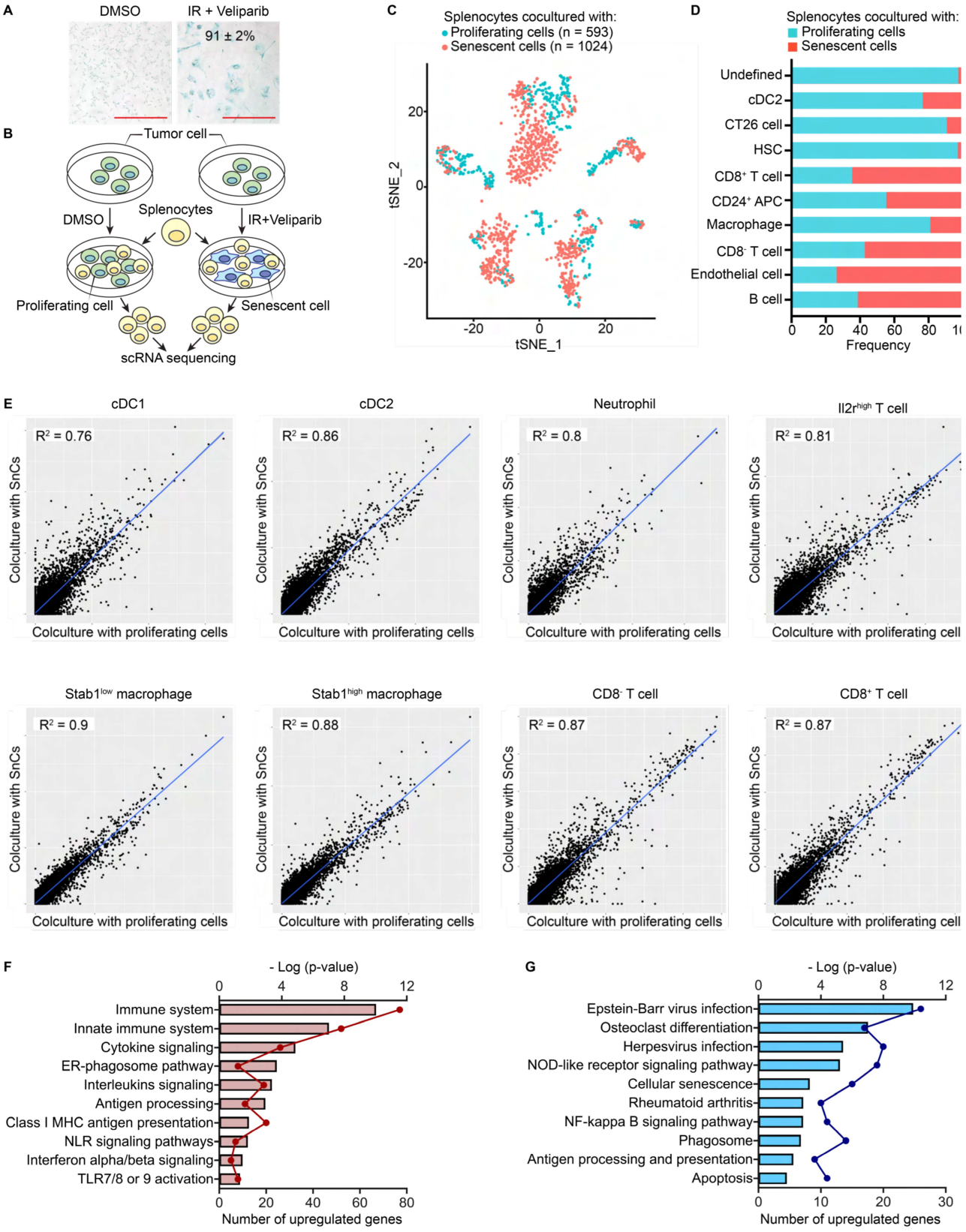
A
DMSO
IR + Veliparib
91 ± 2%
B
Tumor cell
DMSO
Splenocytes
IR+Veliparib
Proliferating cell
Senescent cell
scRNA sequencing
C
Splenocytes cocultured with:
Proliferating cells (n = 593)
Senescent cells (n = 1024)
tSNE_2
tSNE_1
D
Splenocytes cocultured with:
Proliferating cells
Senescent cells
Undefined
cDC2
CT26 cell
HSC
CD8+ T cell
CD24+ APC
Macrophage
CD8- T cell
Endothelial cell
B cell
Frequency
E
cDC1
cDC2
Neutrophil
Il2rhigh T cell
Stab1low macrophage
Stab1high macrophage
CD8- T cell
CD8+ T cell
R² = 0.76
R² = 0.86
R² = 0.8
R² = 0.81
R² = 0.9
R² = 0.88
R² = 0.87
R² = 0.87
Colculture with SnCs
Colculture with proliferating cells
F
- Log (p-value)
Immune system
Innate immune system
Cytokine signaling
ER-phagosome pathway
Interleukins signaling
Antigen processing
Class I MHC antigen presentation
NLR signaling pathways
Interferon alpha/beta signaling
TLR7/8 or 9 activation
Number of upregulated genes
G
- Log (p-value)
Epstein-Barr virus infection
Osteoclast differentiation
Herpesvirus infection
NOD-like receptor signaling pathway
Cellular senescence
Rheumatoid arthritis
NF-kappa B signaling pathway
Phagosome
Antigen processing and presentation
Apoptosis
Number of upregulated genes

Figure S2

A

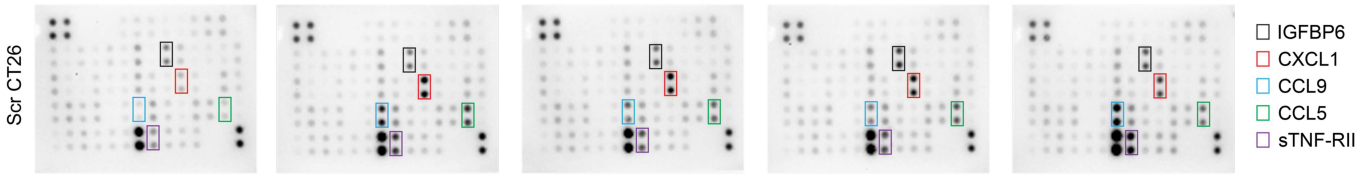

B

	A	B	C	D	E	F	G	H	I	J	K	L	M	N
1	POS	POS	NEG	NEG	Blank	axl	BLC	CD30L	CD30/TNFRSF8	CD40	CRG-2	CTACK	CXCL16	Eotaxin
2	POS	POS	NEG	NEG	Blank	axl	BLC	CD30L	CD30/TNFRSF8	CD40	CRG-2	CTACK	CXCL16	Eotaxin
3	Eotaxin-2	FAS ligand	Fractalkine	G-CSF	GM-CSF	IFN-gamma	IGF-BP-3	IGF-BP-5	IGF-BP-6	IL1-alpha	IL1-beta	IL2	IL3	IL3 Rb
4	Eotaxin-2	FAS ligand	Fractalkine	G-CSF	GM-CSF	IFN-gamma	IGF-BP-3	IGF-BP-5	IGF-BP-6	IL1-alpha	IL1-beta	IL2	IL3	IL3 Rb
5	IL4	IL5	IL6	IL9	IL10	IL12-p40/p70	IL12-p70	IL13	IL17	KC (CXCL1)	Leptin R	Leptin	LIX (CXCL5)	L-Selectin
6	IL4	IL5	IL6	IL9	IL10	IL12-p40/p70	IL12-p70	IL13	IL17	KC (CXCL1)	Leptin R	Leptin	LIX (CXCL5)	L-Selectin
7	Lymphotactin	MCP-1	MCP-5	M-CSF	MIG (CXCL9)	MIP-1-alpha	MIP-1-gamma (CCL9)	MIP-2	MIP-3-beta	MIP-3-alpha (CCL20)	PF4	P-Selectin	RANTES (CCL5)	SCF
8	Lymphotactin	MCP-1	MCP-5	M-CSF	MIG (CXCL9)	MIP-1-alpha	MIP-1-gamma (CCL9)	MIP-2	MIP-3-beta	MIP-3-alpha (CCL20)	PF4	P-Selectin	RANTES (CCL5)	SCF
9	SDF-1-alpha	TARC	TCA-3	TECK	TIMP-1	TNF-alpha	sTNF RI	sTNF RII	TPO	VCAM-1	VEGF	Blank	Blank	POS
10	SDF-1-alpha	TARC	TCA-3	TECK	TIMP-1	TNF-alpha	sTNF RI	sTNF RII	TPO	VCAM-1	VEGF	Blank	Blank	POS

Figure S3

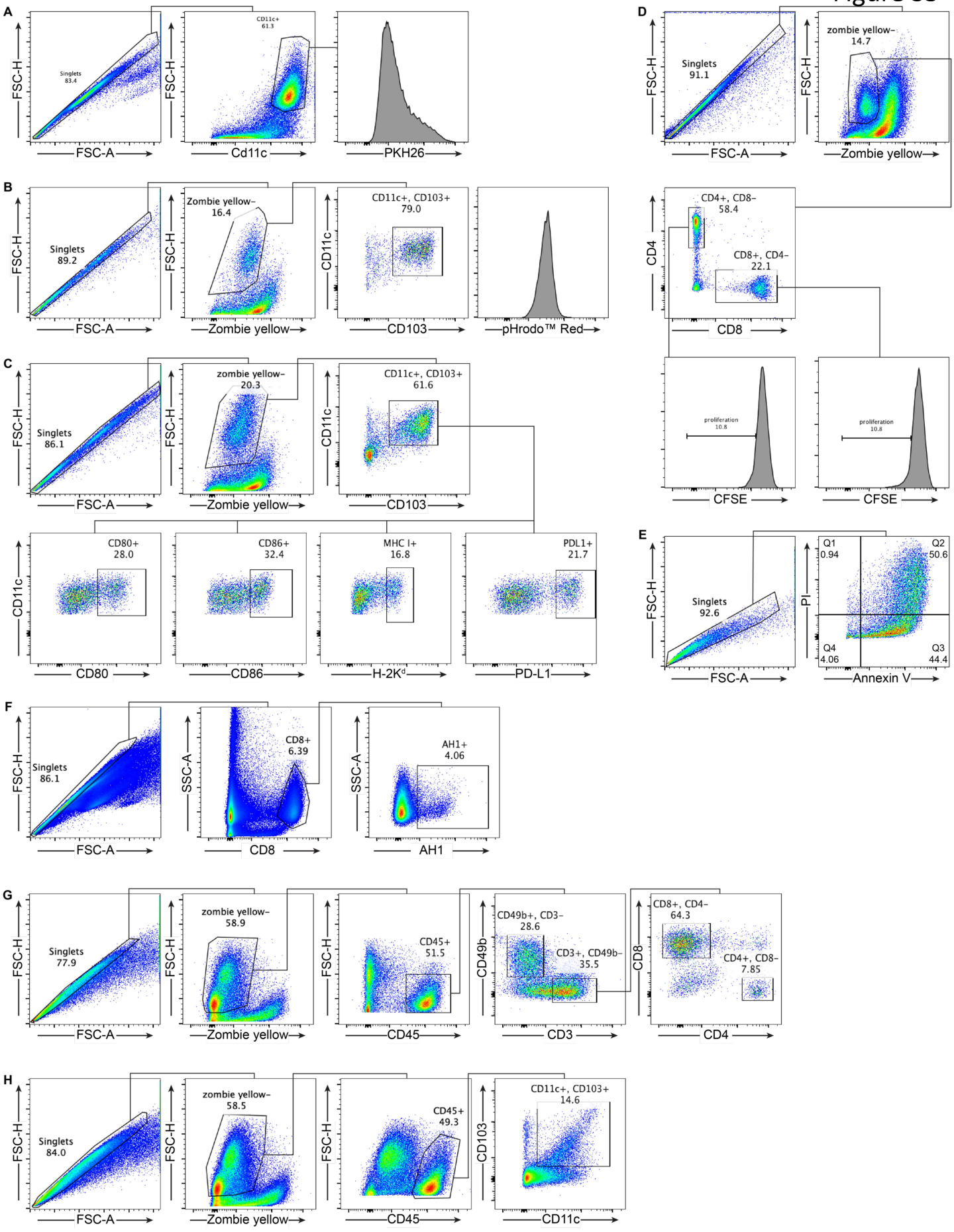
A
FSC-H
FSC-A
Singlets
83.4
CD11c+
61.3
Cd11c
PKH26
B
Singlets
89.2
Zombie yellow–
16.4
CD11c+, CD103+
79.0
CD11c
CD103
pHrodo™ Red
C
Singlets
86.1
zombie yellow–
20.3
CD11c+, CD103+
61.6
CD80+
28.0
CD86+
32.4
MHC I+
16.8
PDL1+
21.7
CD80
CD86
H-2K^d
PD-L1
D
Singlets
91.1
zombie yellow–
14.7
Zombie yellow
CD4+, CD8–
58.4
CD8+, CD4–
22.1
CD4
CD8
proliferation
10.8
CFSE
E
Singlets
92.6
Q1
0.94
Q2
50.6
Q4
4.06
Q3
44.4
PI
Annexin V
F
Singlets
86.1
CD8+
6.39
AH1+
4.06
SSC-A
AH1
G
Singlets
77.9
zombie yellow–
58.9
CD45+
51.5
CD49b+, CD3–
28.6
CD3+, CD49b–
35.5
CD8+, CD4–
64.3
CD4+, CD8–
7.85
CD49b
CD45
CD3
CD8
CD4
H
Singlets
84.0
zombie yellow–
58.5
CD45+
49.3
CD11c+, CD103+
14.6

Figure S4

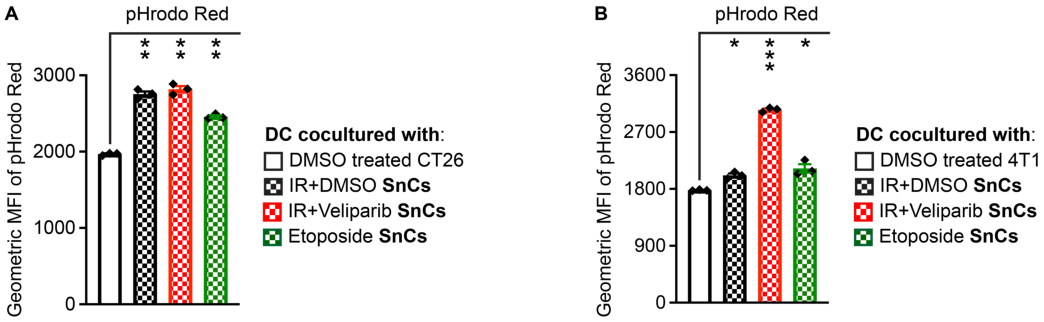
A
pHrodo Red
Geometric MFI of pHrodo Red
3000
2000
1000
0
DC cocultured with:
DMSO treated CT26
IR+DMSO SnCs
IR+Veliparib SnCs
Etoposide SnCs
B
pHrodo Red
Geometric MFI of pHrodo Red
3600
2700
1800
900
0
DC cocultured with:
DMSO treated 4T1
IR+DMSO SnCs
IR+Veliparib SnCs
Etoposide SnCs

Figure S5

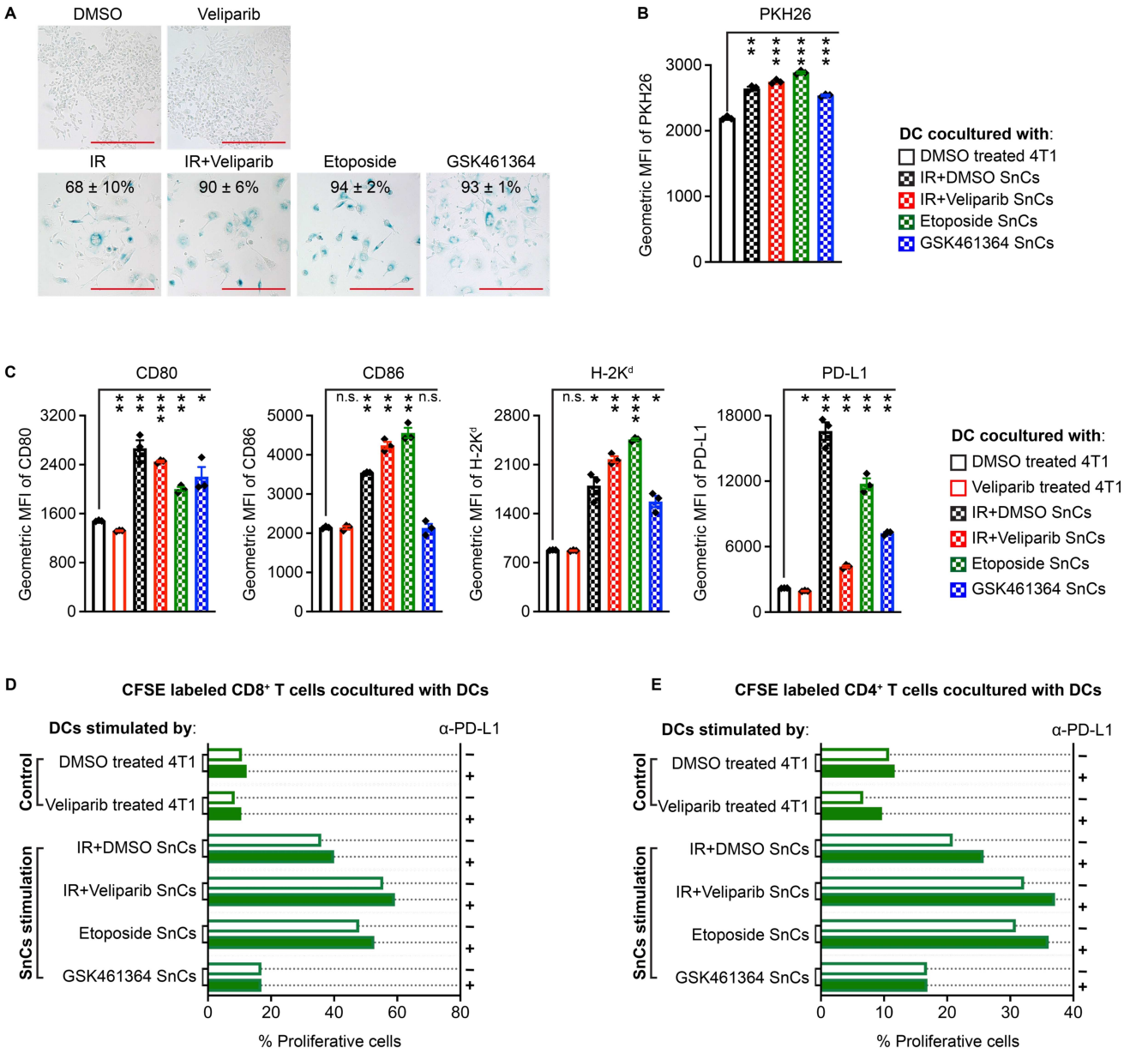
A
DMSO
Veliparib
IR
68 ± 10%
IR+Veliparib
90 ± 6%
Etoposide
94 ± 2%
GSK461364
93 ± 1%
B
PKH26
Geometric MFI of PKH26
DC cocultured with:
DMSO treated 4T1
IR+DMSO SnCs
IR+Veliparib SnCs
Etoposide SnCs
GSK461364 SnCs
C
CD80
CD86
H-2Kd
PD-L1
Geometric MFI of CD80
Geometric MFI of CD86
Geometric MFI of H-2Kd
Geometric MFI of PD-L1
n.s.
DC cocultured with:
DMSO treated 4T1
Veliparib treated 4T1
IR+DMSO SnCs
IR+Veliparib SnCs
Etoposide SnCs
GSK461364 SnCs
D
CFSE labeled CD8+ T cells cocultured with DCs
DCs stimulated by:
α-PD-L1
Control
DMSO treated 4T1
Veliparib treated 4T1
SnCs stimulation
IR+DMSO SnCs
IR+Veliparib SnCs
Etoposide SnCs
GSK461364 SnCs
% Proliferative cells
E
CFSE labeled CD4+ T cells cocultured with DCs
DCs stimulated by:
α-PD-L1
Control
DMSO treated 4T1
Veliparib treated 4T1
SnCs stimulation
IR+DMSO SnCs
IR+Veliparib SnCs
Etoposide SnCs
GSK461364 SnCs
% Proliferative cells

Figure S6

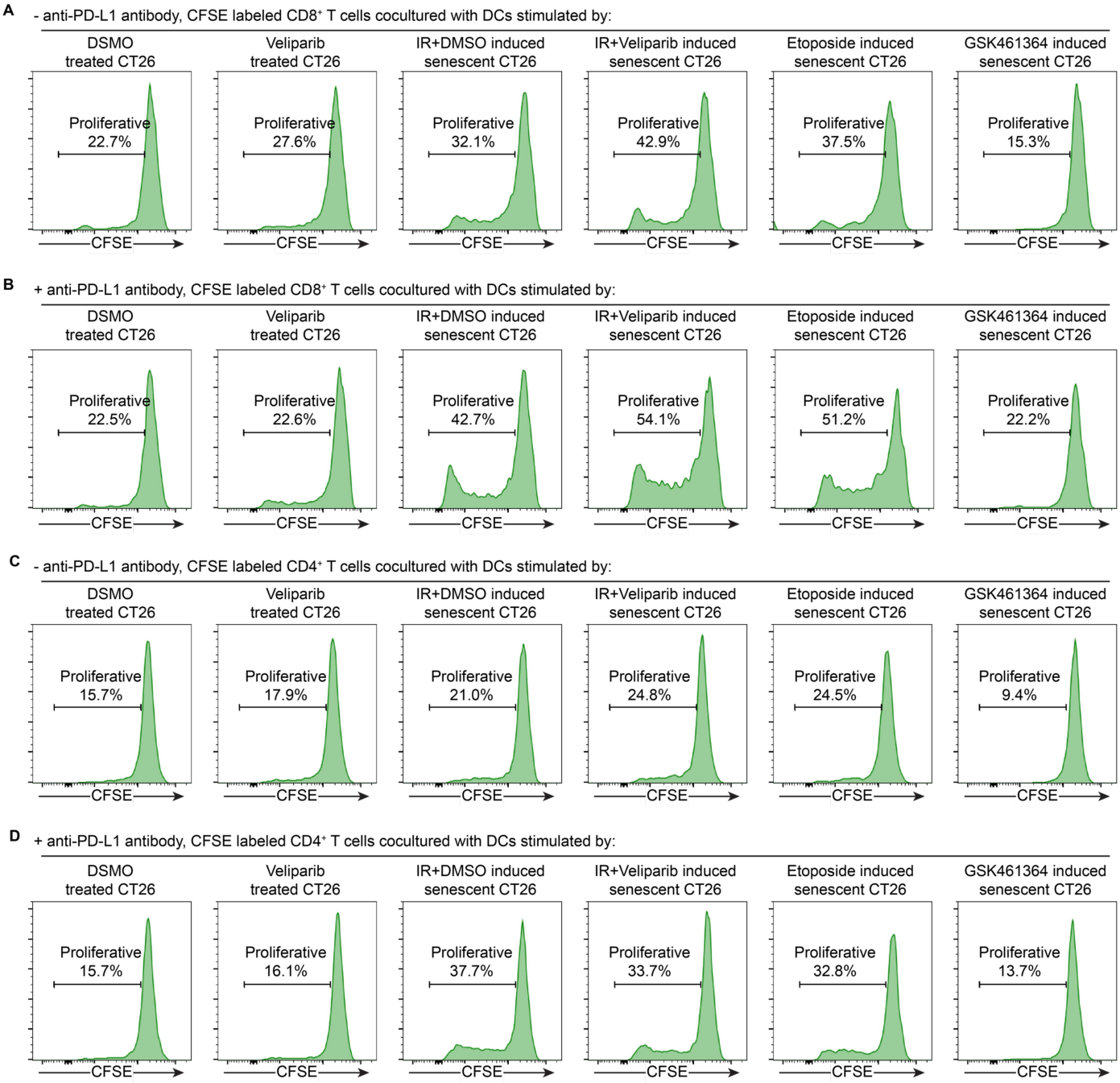
A
- anti-PD-L1 antibody, CFSE labeled CD8+ T cells cocultured with DCs stimulated by:
DSMO treated CT26
Proliferative 22.7%
Veliparib treated CT26
Proliferative 27.6%
IR+DMSO induced senescent CT26
Proliferative 32.1%
IR+Veliparib induced senescent CT26
Proliferative 42.9%
Etoposide induced senescent CT26
Proliferative 37.5%
GSK461364 induced senescent CT26
Proliferative 15.3%
CFSE
B
+ anti-PD-L1 antibody, CFSE labeled CD8+ T cells cocultured with DCs stimulated by:
DSMO treated CT26
Proliferative 22.5%
Veliparib treated CT26
Proliferative 22.6%
IR+DMSO induced senescent CT26
Proliferative 42.7%
IR+Veliparib induced senescent CT26
Proliferative 54.1%
Etoposide induced senescent CT26
Proliferative 51.2%
GSK461364 induced senescent CT26
Proliferative 22.2%
CFSE
C
- anti-PD-L1 antibody, CFSE labeled CD4+ T cells cocultured with DCs stimulated by:
DSMO treated CT26
Proliferative 15.7%
Veliparib treated CT26
Proliferative 17.9%
IR+DMSO induced senescent CT26
Proliferative 21.0%
IR+Veliparib induced senescent CT26
Proliferative 24.8%
Etoposide induced senescent CT26
Proliferative 24.5%
GSK461364 induced senescent CT26
Proliferative 9.4%
CFSE
D
+ anti-PD-L1 antibody, CFSE labeled CD4+ T cells cocultured with DCs stimulated by:
DSMO treated CT26
Proliferative 15.7%
Veliparib treated CT26
Proliferative 16.1%
IR+DMSO induced senescent CT26
Proliferative 37.7%
IR+Veliparib induced senescent CT26
Proliferative 33.7%
Etoposide induced senescent CT26
Proliferative 32.8%
GSK461364 induced senescent CT26
Proliferative 13.7%
CFSE

Figure S7

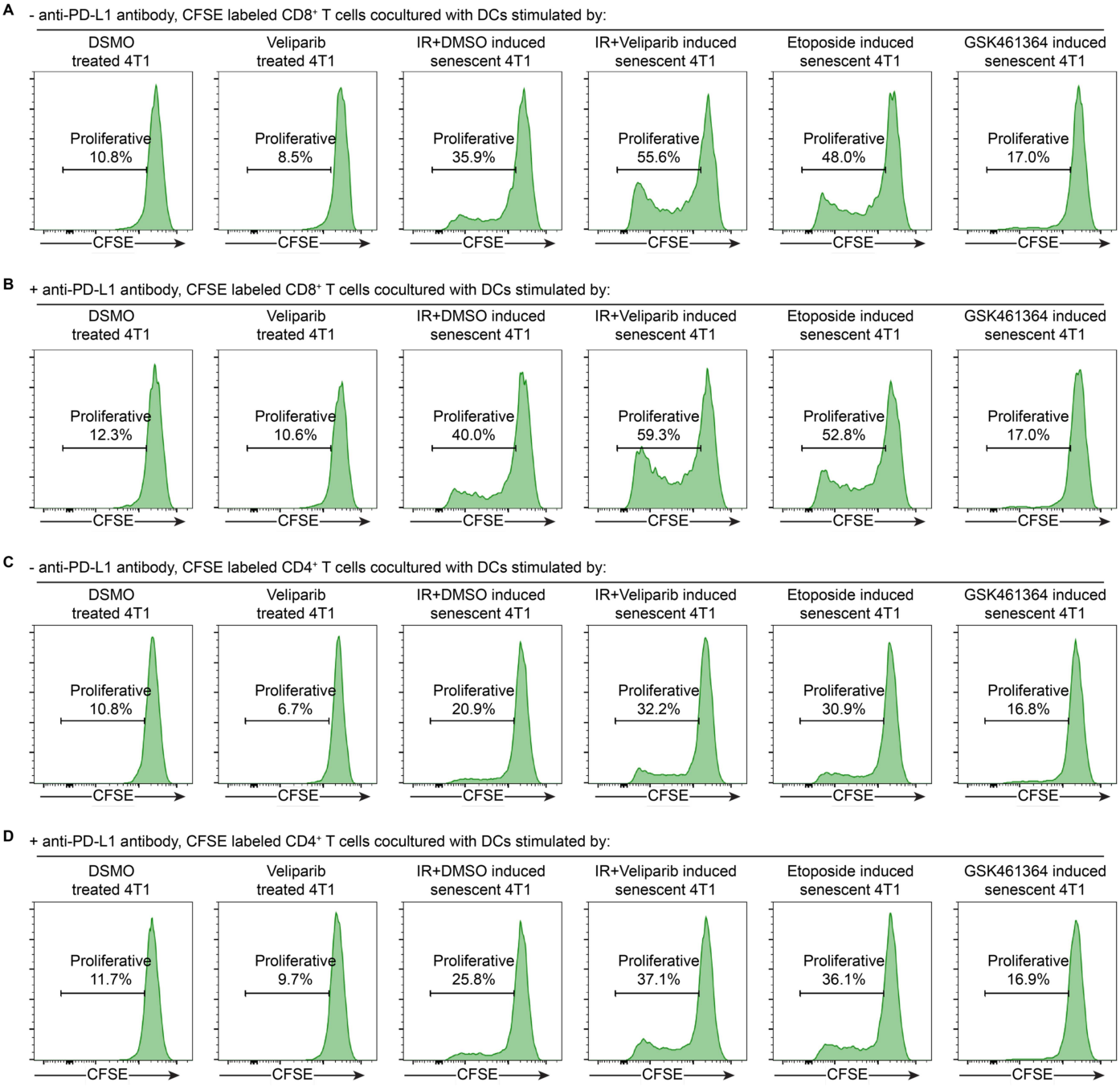
A
- anti-PD-L1 antibody, CFSE labeled CD8+ T cells cocultured with DCs stimulated by:
DSMO treated 4T1
Veliparib treated 4T1
IR+DMSO induced senescent 4T1
IR+Veliparib induced senescent 4T1
Etoposide induced senescent 4T1
GSK461364 induced senescent 4T1
Proliferative 10.8%
Proliferative 8.5%
Proliferative 35.9%
Proliferative 55.6%
Proliferative 48.0%
Proliferative 17.0%
CFSE
B
+ anti-PD-L1 antibody, CFSE labeled CD8+ T cells cocultured with DCs stimulated by:
DSMO treated 4T1
Veliparib treated 4T1
IR+DMSO induced senescent 4T1
IR+Veliparib induced senescent 4T1
Etoposide induced senescent 4T1
GSK461364 induced senescent 4T1
Proliferative 12.3%
Proliferative 10.6%
Proliferative 40.0%
Proliferative 59.3%
Proliferative 52.8%
Proliferative 17.0%
CFSE
C
- anti-PD-L1 antibody, CFSE labeled CD4+ T cells cocultured with DCs stimulated by:
DSMO treated 4T1
Veliparib treated 4T1
IR+DMSO induced senescent 4T1
IR+Veliparib induced senescent 4T1
Etoposide induced senescent 4T1
GSK461364 induced senescent 4T1
Proliferative 10.8%
Proliferative 6.7%
Proliferative 20.9%
Proliferative 32.2%
Proliferative 30.9%
Proliferative 16.8%
CFSE
D
+ anti-PD-L1 antibody, CFSE labeled CD4+ T cells cocultured with DCs stimulated by:
DSMO treated 4T1
Veliparib treated 4T1
IR+DMSO induced senescent 4T1
IR+Veliparib induced senescent 4T1
Etoposide induced senescent 4T1
GSK461364 induced senescent 4T1
Proliferative 11.7%
Proliferative 9.7%
Proliferative 25.8%
Proliferative 37.1%
Proliferative 36.1%
Proliferative 16.9%
CFSE

Figure S8

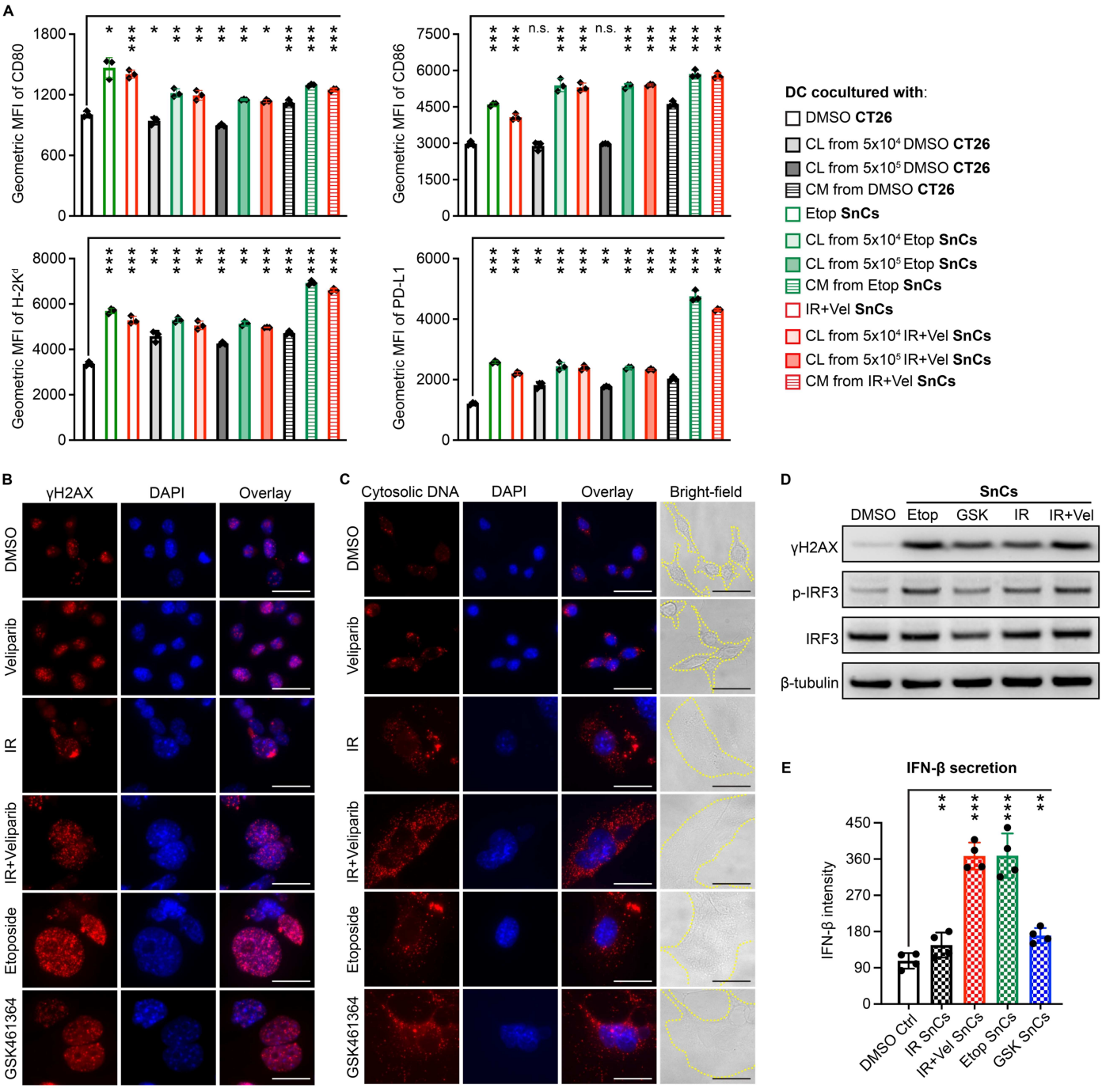
A
Geometric MFI of CD80
Geometric MFI of CD86
Geometric MFI of H-2K^d
Geometric MFI of PD-L1
n.s.
DC cocultured with:
DMSO CT26
CL from 5x10^4 DMSO CT26
CL from 5x10^5 DMSO CT26
CM from DMSO CT26
Etop SnCs
CL from 5x10^4 Etop SnCs
CL from 5x10^5 Etop SnCs
CM from Etop SnCs
IR+Vel SnCs
CL from 5x10^4 IR+Vel SnCs
CL from 5x10^5 IR+Vel SnCs
CM from IR+Vel SnCs
B
γH2AX
DAPI
Overlay
DMSO
Veliparib
IR
IR+Veliparib
Etoposide
GSK461364
C
Cytosolic DNA
DAPI
Overlay
Bright-field
D
SnCs
DMSO
Etop
GSK
IR
IR+Vel
γH2AX
p-IRF3
IRF3
β-tubulin
E
IFN-β secretion
IFN-β intensity
DMSO Ctrl
IR SnCs
IR+Vel SnCs
Etop SnCs
GSK SnCs

Figure S9

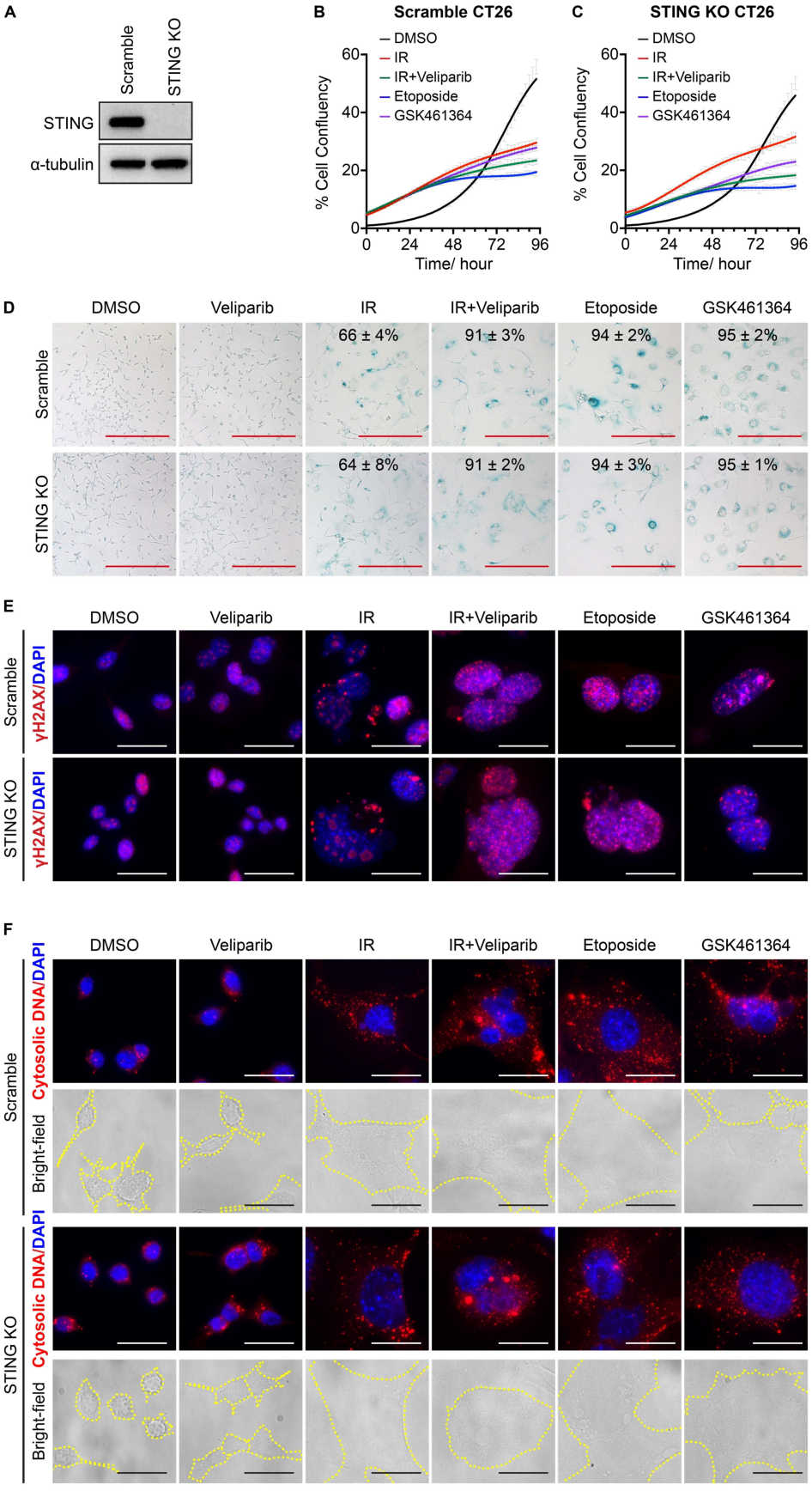
A
Scramble
STING KO
STING
α-tubulin
B
Scramble CT26
DMSO
IR
IR+Veliparib
Etoposide
GSK461364
% Cell Confluency
Time/ hour
C
STING KO CT26
D
DMSO
Veliparib
IR
IR+Veliparib
Etoposide
GSK461364
66 ± 4%
91 ± 3%
94 ± 2%
95 ± 2%
64 ± 8%
91 ± 2%
94 ± 3%
95 ± 1%
E
γH2AX/DAPI
F
Cytosolic DNA/DAPI
Bright-field

Figure S10

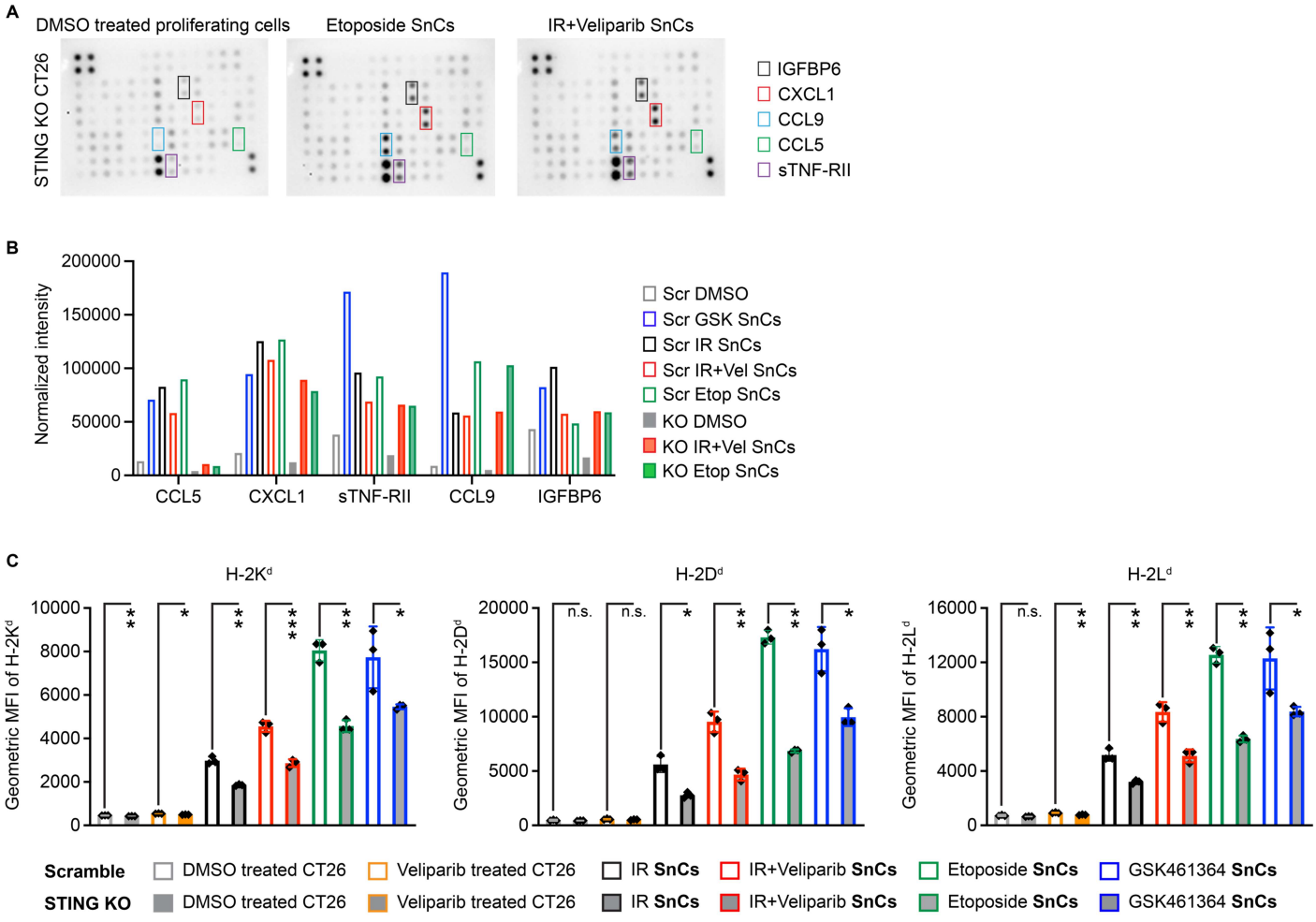
A
DMSO treated proliferating cells
Etoposide SnCs
IR+Veliparib SnCs
STING KO CT26
IGFBP6
CXCL1
CCL9
CCL5
sTNF-RII
B
Normalized intensity
200000
150000
100000
50000
0
CCL5
CXCL1
sTNF-RII
CCL9
IGFBP6
Scr DMSO
Scr GSK SnCs
Scr IR SnCs
Scr IR+Vel SnCs
Scr Etop SnCs
KO DMSO
KO IR+Vel SnCs
KO Etop SnCs
C
H-2Kd
H-2Dd
H-2Ld
Geometric MFI of H-2Kd
Geometric MFI of H-2Dd
Geometric MFI of H-2Ld
n.s.
Scramble
STING KO
DMSO treated CT26
Veliparib treated CT26
IR SnCs
IR+Veliparib SnCs
Etoposide SnCs
GSK461364 SnCs

Figure S11

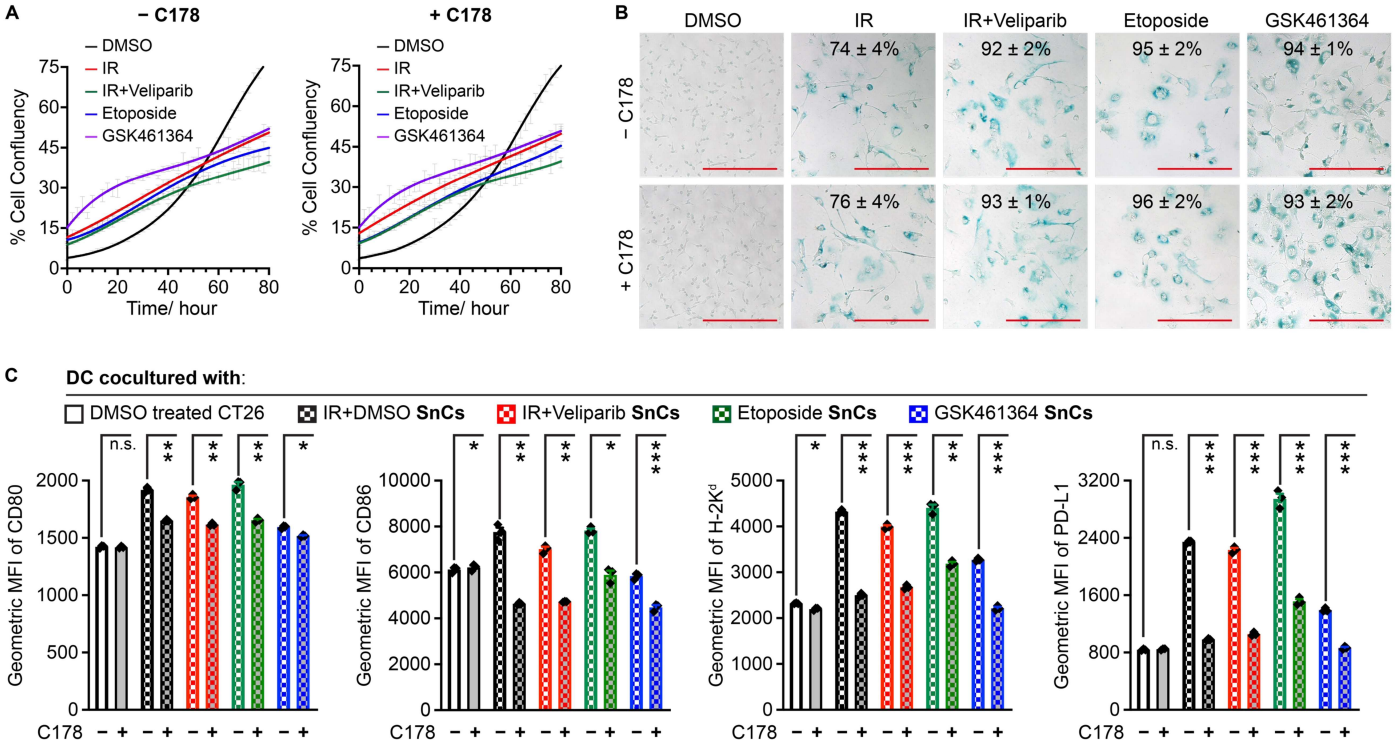
A
− C178
+ C178
DMSO
IR
IR+Veliparib
Etoposide
GSK461364
% Cell Confluency
Time/ hour
B
DMSO
IR
IR+Veliparib
Etoposide
GSK461364
− C178
+ C178
74 ± 4%
92 ± 2%
95 ± 2%
94 ± 1%
76 ± 4%
93 ± 1%
96 ± 2%
93 ± 2%
C
DC cocultured with:
DMSO treated CT26
IR+DMSO SnCs
IR+Veliparib SnCs
Etoposide SnCs
GSK461364 SnCs
Geometric MFI of CD80
Geometric MFI of CD86
Geometric MFI of H-2K^{d}
Geometric MFI of PD-L1
n.s.
C178

Figure S12

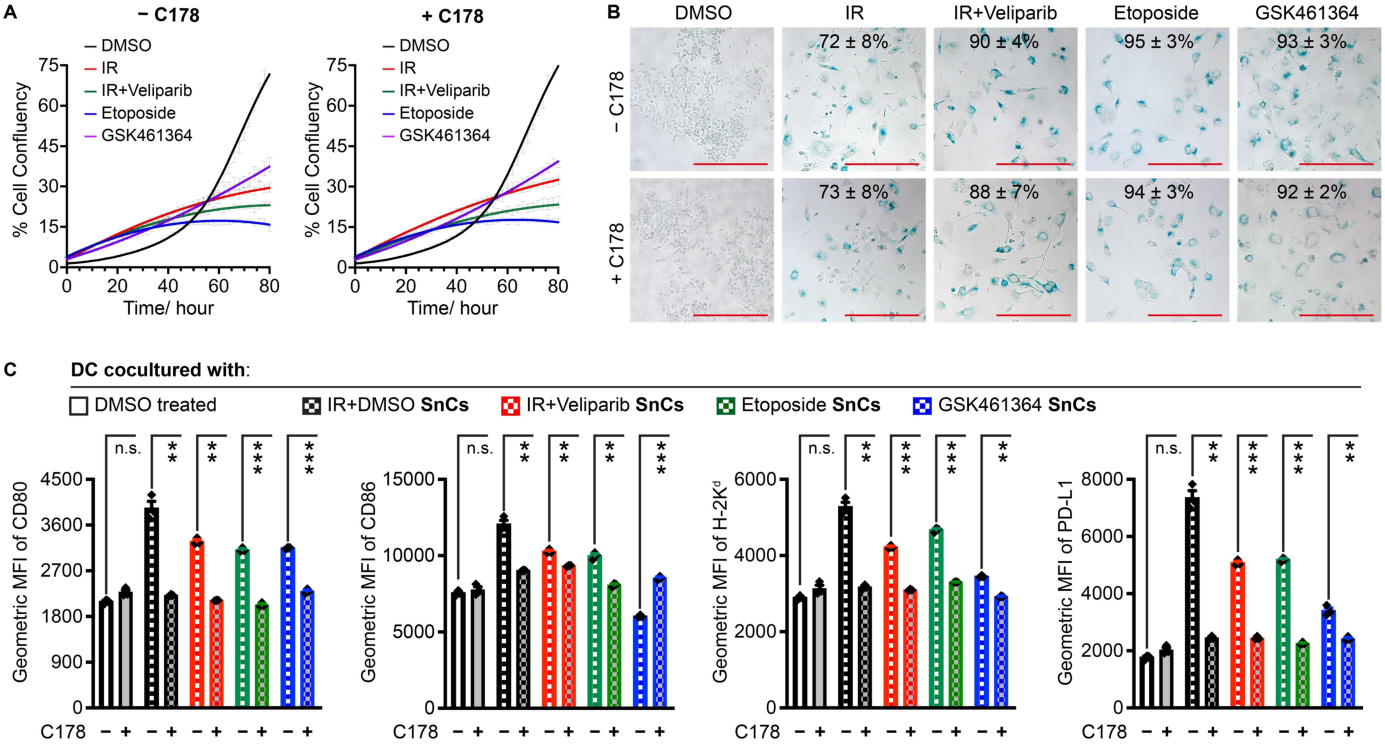
A
− C178
+ C178
DMSO
IR
IR+Veliparib
Etoposide
GSK461364
% Cell Confluency
Time/ hour
B
DMSO
IR
IR+Veliparib
Etoposide
GSK461364
− C178
+ C178
72 ± 8%
90 ± 4%
95 ± 3%
93 ± 3%
73 ± 8%
88 ± 7%
94 ± 3%
92 ± 2%
C
DC cocultured with:
DMSO treated
IR+DMSO SnCs
IR+Veliparib SnCs
Etoposide SnCs
GSK461364 SnCs
Geometric MFI of CD80
Geometric MFI of CD86
Geometric MFI of H-2Kd
Geometric MFI of PD-L1
n.s.
C178

Figure S13

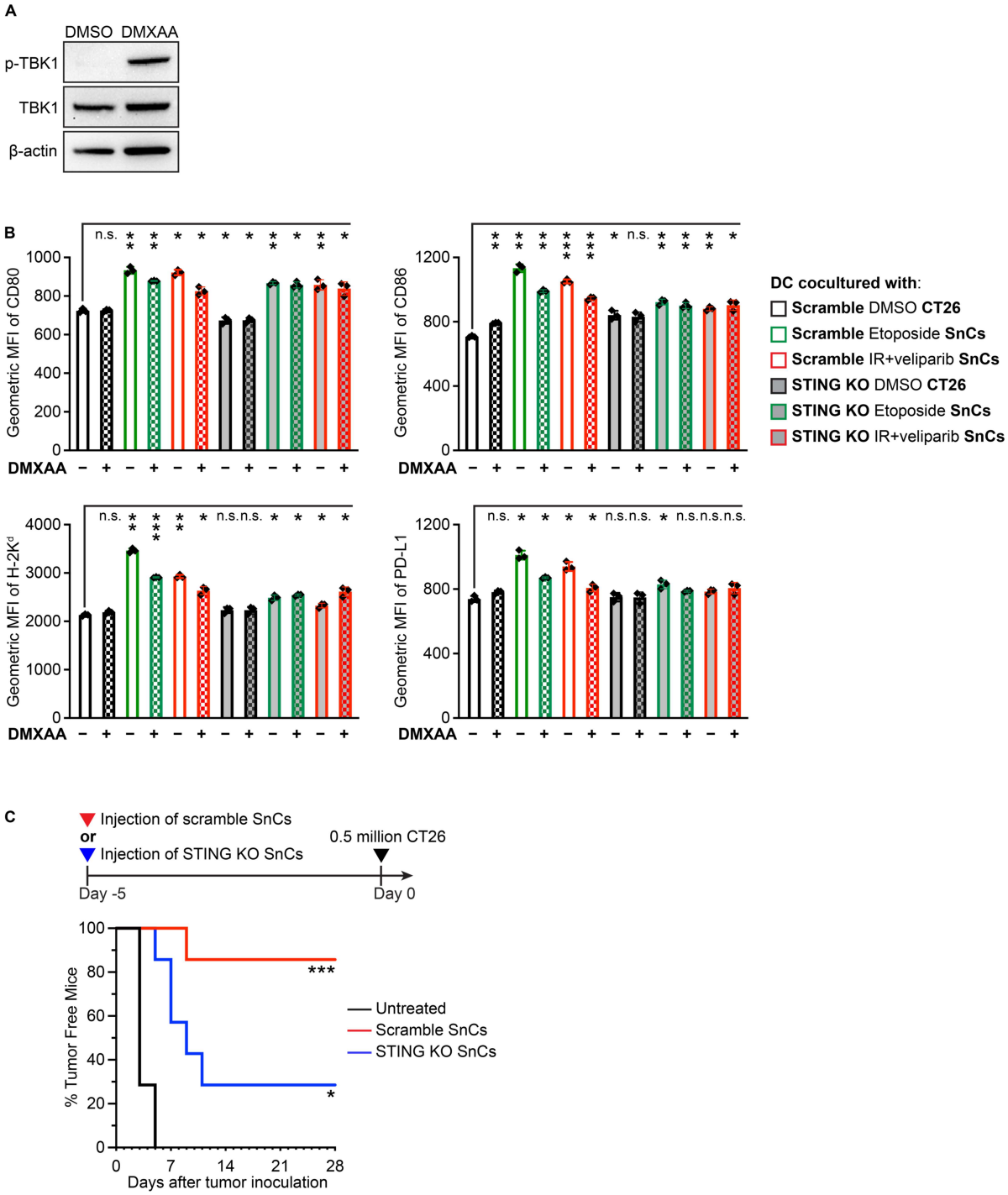
A
DMSO DMXAA
p-TBK1
TBK1
β-actin
B
Geometric MFI of CD80
Geometric MFI of CD86
Geometric MFI of H-2K^d
Geometric MFI of PD-L1
DMXAA
DC cocultured with:
Scramble DMSO CT26
Scramble Etoposide SnCs
Scramble IR+veliparib SnCs
STING KO DMSO CT26
STING KO Etoposide SnCs
STING KO IR+veliparib SnCs
C
Injection of scramble SnCs
or
Injection of STING KO SnCs
0.5 million CT26
Day -5
Day 0
% Tumor Free Mice
Days after tumor inoculation
Untreated
Scramble SnCs
STING KO SnCs

Figure S14

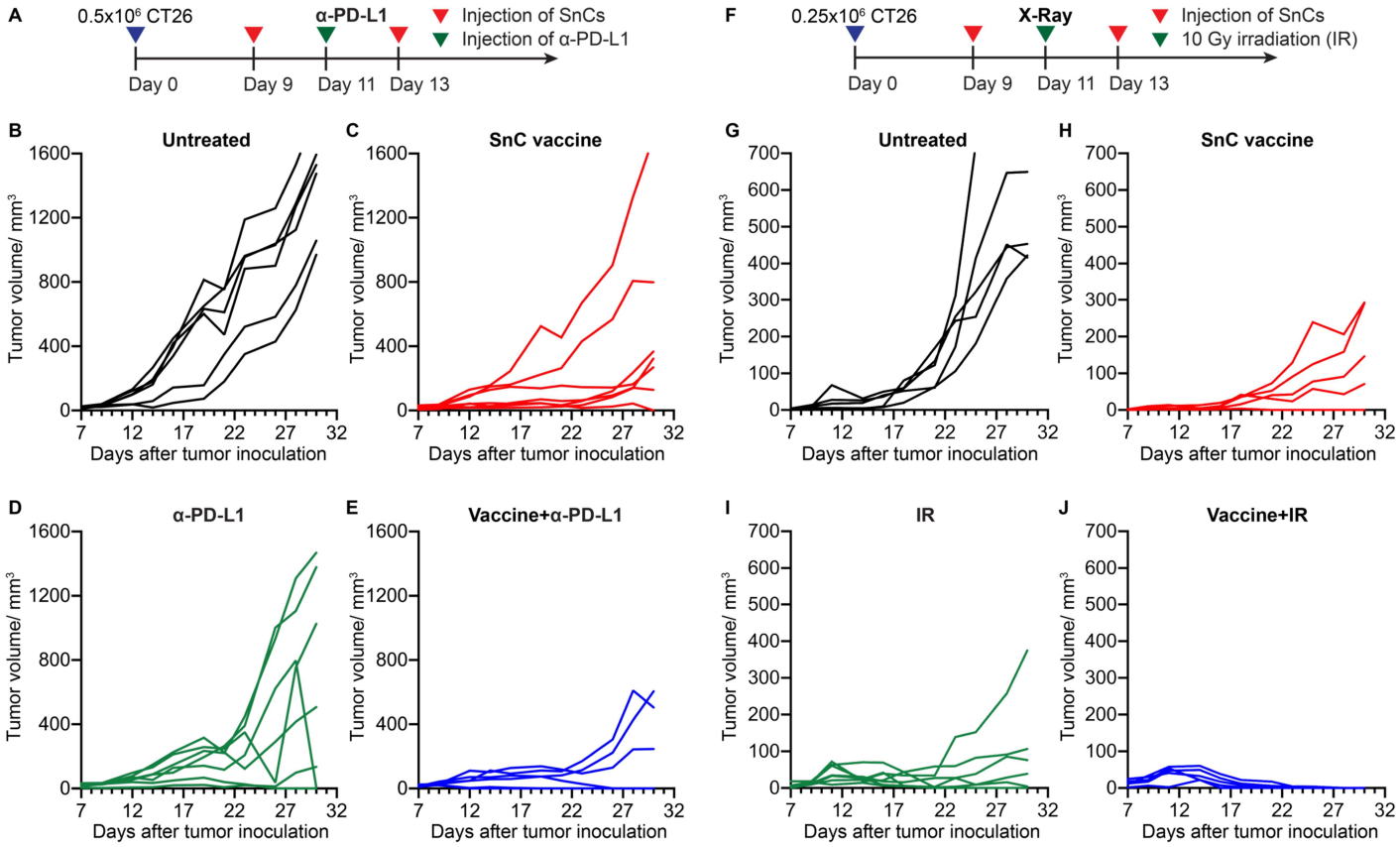
A
0.5x10⁶ CT26
α-PD-L1
Injection of SnCs
Injection of α-PD-L1
Day 0
Day 9
Day 11
Day 13
F
0.25x10⁶ CT26
X-Ray
Injection of SnCs
10 Gy irradiation (IR)
Day 0
Day 9
Day 11
Day 13
B
Untreated
C
SnC vaccine
G
Untreated
H
SnC vaccine
D
α-PD-L1
E
Vaccine+α-PD-L1
I
IR
J
Vaccine+IR
Tumor volume/ mm³
Days after tumor inoculation

Figure S15

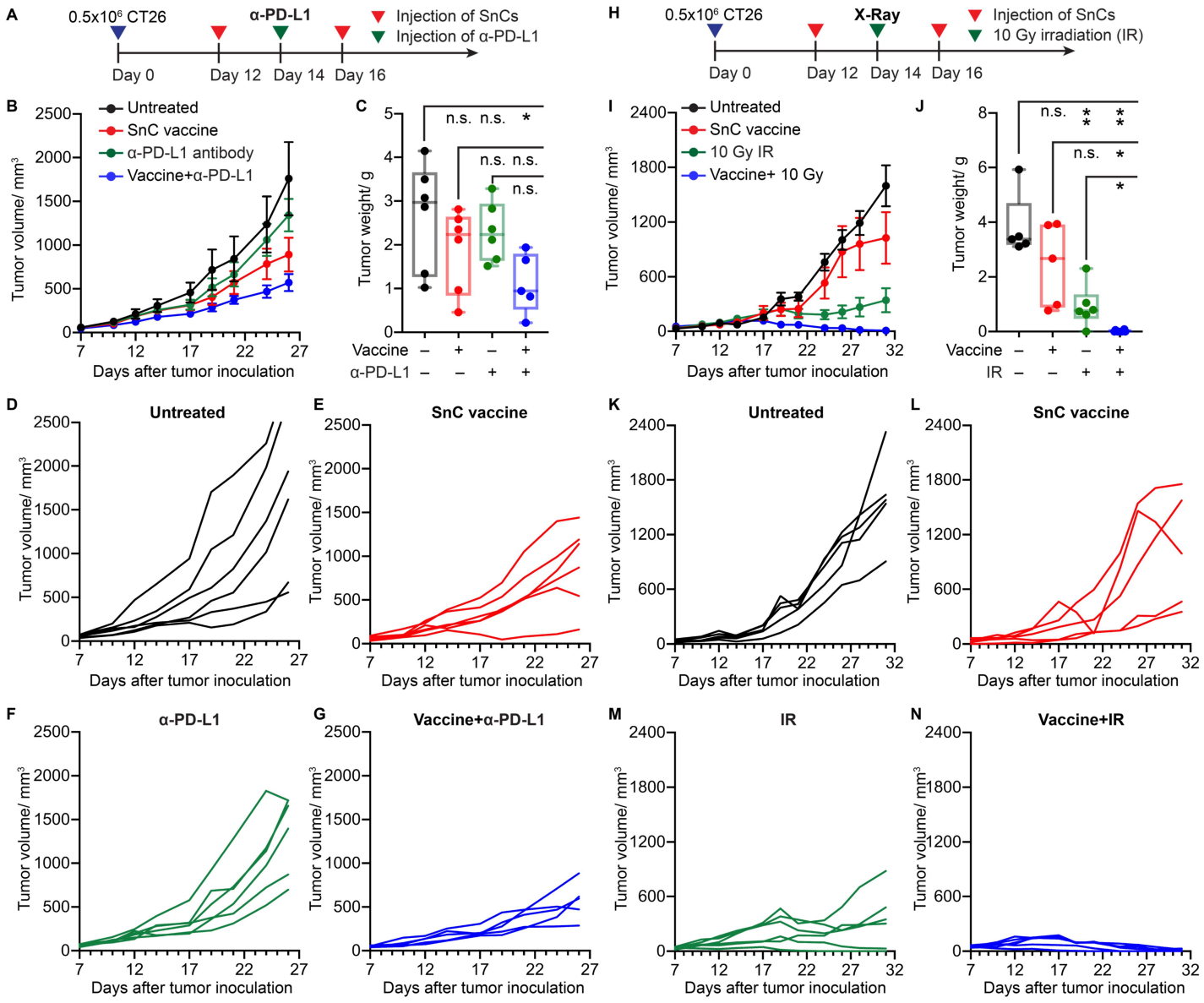
A
0.5x10⁶ CT26
α-PD-L1
Injection of SnCs
Injection of α-PD-L1
Day 0
Day 12
Day 14
Day 16
B
Untreated
SnC vaccine
α-PD-L1 antibody
Vaccine+α-PD-L1
Tumor volume/ mm³
Days after tumor inoculation
C
Tumor weight/ g
n.s.
*
Vaccine
α-PD-L1
H
0.5x10⁶ CT26
X-Ray
Injection of SnCs
10 Gy irradiation (IR)
I
Untreated
SnC vaccine
10 Gy IR
Vaccine+ 10 Gy
J
IR
D
Untreated
E
SnC vaccine
K
L
F
α-PD-L1
G
Vaccine+α-PD-L1
M
IR
N
Vaccine+IR

Figure S16

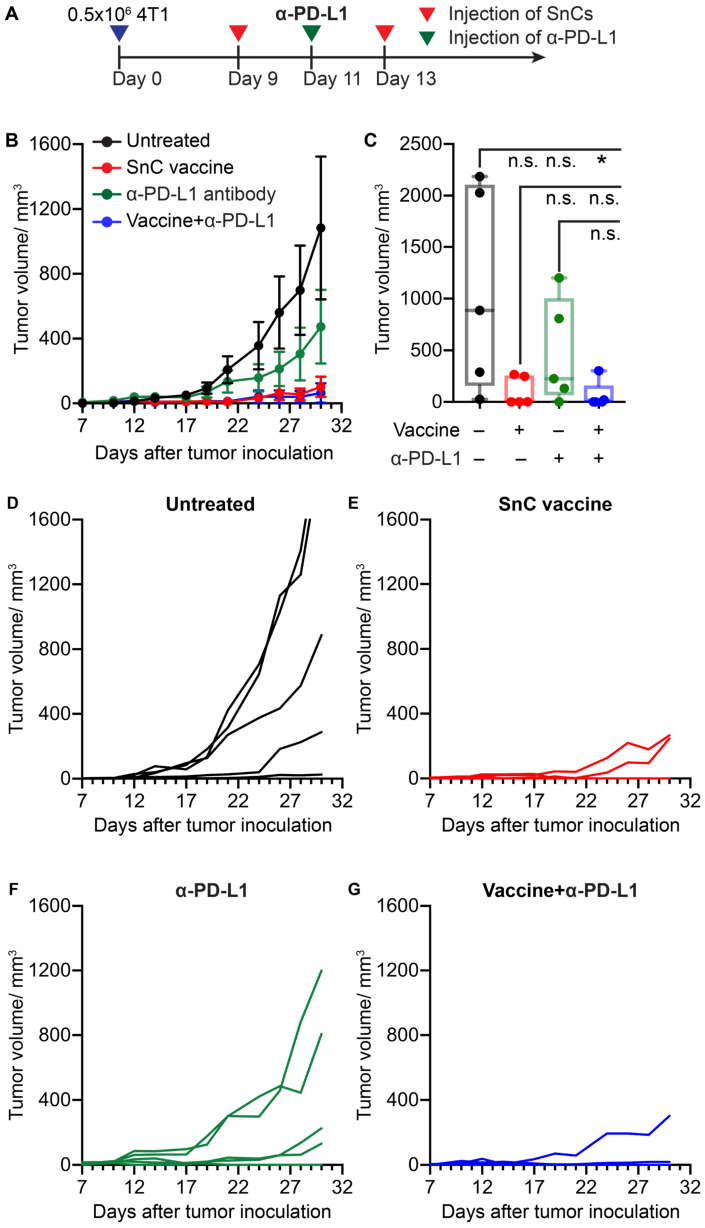
A
0.5x10⁶ 4T1
α-PD-L1
Injection of SnCs
Injection of α-PD-L1
Day 0
Day 9
Day 11
Day 13
B
Untreated
SnC vaccine
α-PD-L1 antibody
Vaccine+α-PD-L1
Tumor volume/ mm³
Days after tumor inoculation
C
n.s.
*
Vaccine
α-PD-L1
D
Untreated
E
SnC vaccine
F
α-PD-L1
G
Vaccine+α-PD-L1

Figure S17

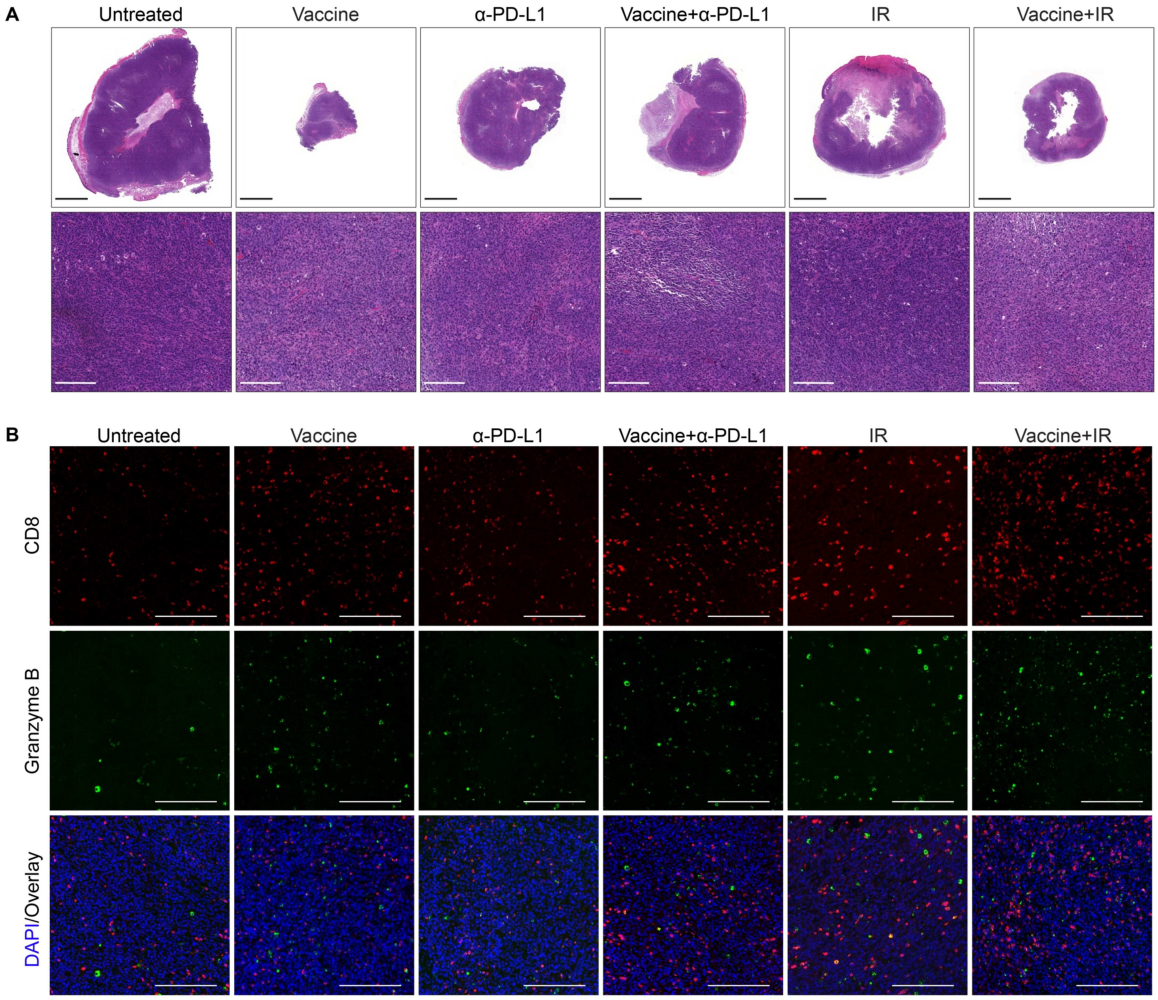
A
Untreated
Vaccine
α-PD-L1
Vaccine+α-PD-L1
IR
Vaccine+IR
B
Untreated
Vaccine
α-PD-L1
Vaccine+α-PD-L1
IR
Vaccine+IR
CD8
Granzyme B
DAPI/Overlay

Figure S18

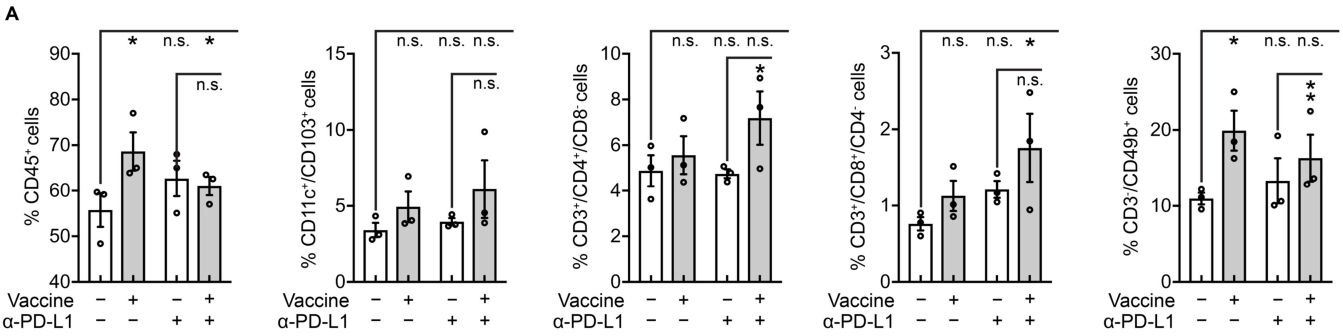
A
% CD45+ cells
% CD11c+/CD103+ cells
% CD3+/CD4+/CD8- cells
% CD3+/CD8+/CD4- cells
% CD3-/CD49b+ cells
Vaccine
α-PD-L1
n.s.

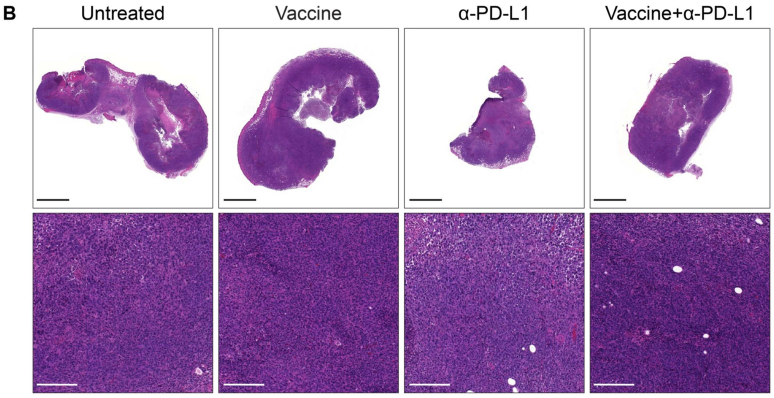
B
Untreated
Vaccine
α-PD-L1
Vaccine+α-PD-L1

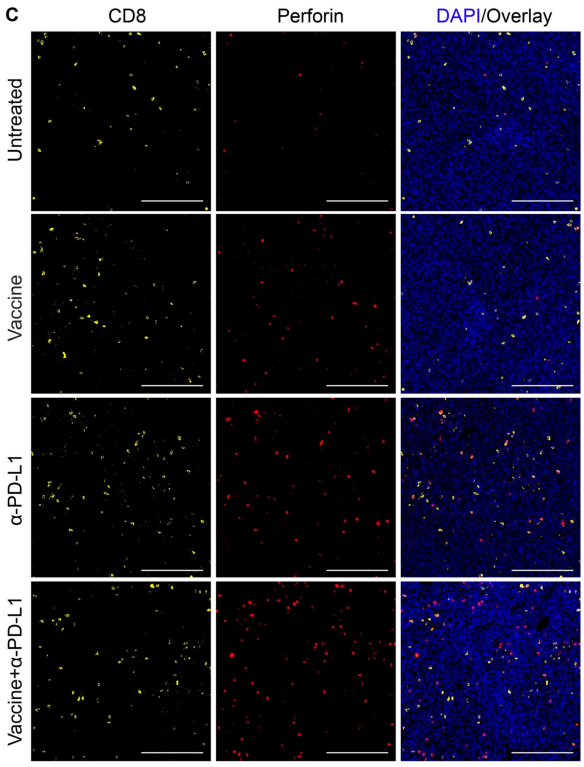
C
CD8
Perforin
DAPI/Overlay
Untreated
Vaccine
α-PD-L1
Vaccine+α-PD-L1

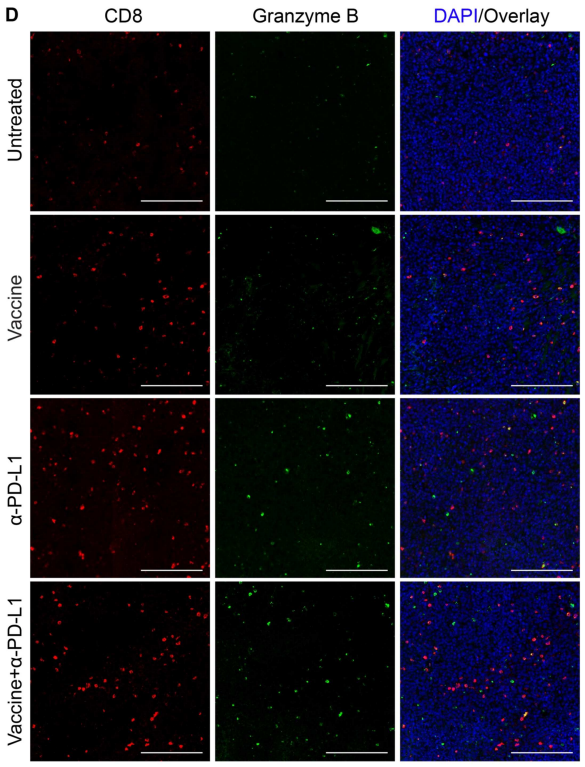
D
CD8
Granzyme B
DAPI/Overlay
Untreated
Vaccine
α-PD-L1
Vaccine+α-PD-L1

Figure S19

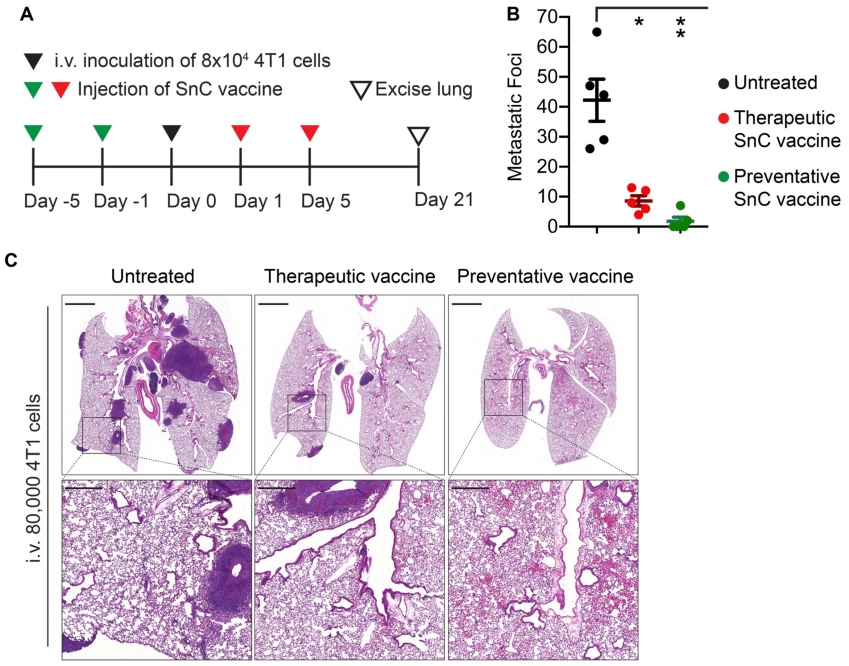
A
i.v. inoculation of 8x10⁴ 4T1 cells
Injection of SnC vaccine
Excise lung
Day -5
Day -1
Day 0
Day 1
Day 5
Day 21
B
Metastatic Foci
70
60
50
40
30
20
10
0
*
**
Untreated
Therapeutic SnC vaccine
Preventative SnC vaccine
C
Untreated
Therapeutic vaccine
Preventative vaccine
i.v. 80,000 4T1 cells

Figure S20

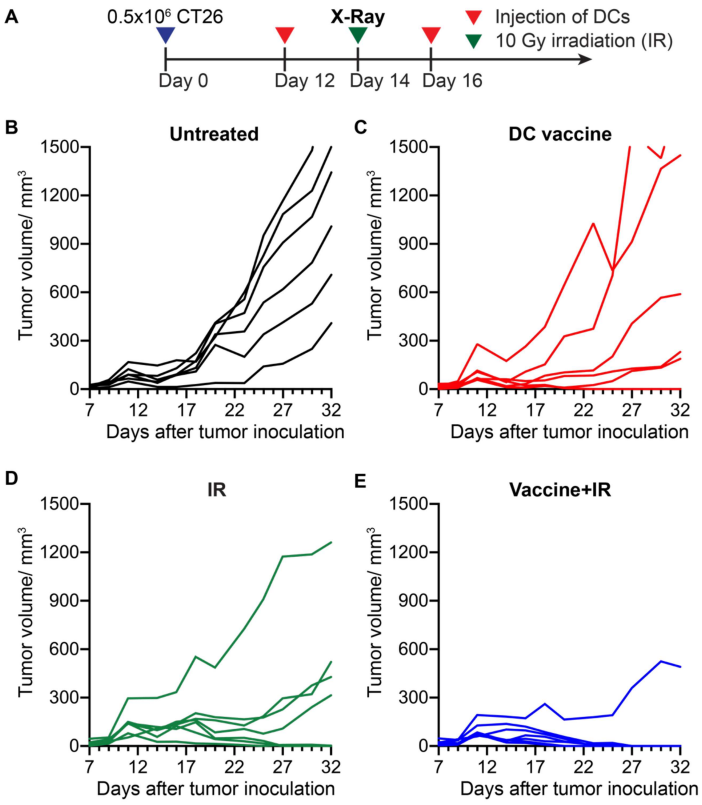
A
0.5x10⁶ CT26
X-Ray
Injection of DCs
10 Gy irradiation (IR)
Day 0
Day 12
Day 14
Day 16
B
Untreated
C
DC vaccine
D
IR
E
Vaccine+IR
Tumor volume/ mm³
Days after tumor inoculation
0
300
600
900
1200
1500
7
12
17
22
27
32

Supplementary information

Senescent cancer cell vaccines induce cytotoxic T cell responses targeting primary tumors and disseminated tumor cells

Yue Liu[1]†, Joanna Pagacz[1]†, Donald J. Wolfgeher[1], Kenneth D. Bromberg[2], Jacob V. Gorman[2], Stephen J. Kron[1]

[1]Ludwig Center for Metastasis Research and Department of Molecular Genetics and Cell Biology, The University of Chicago, Chicago IL

[2]Oncology Discovery, AbbVie, North Chicago IL

Correspondence: skron@uchicago.edu (SJK)

† These authors contributed equally to this work.

The PDF file includes:

Supplementary methods

Fig. S1 to S20

Table S1 and S2

Supplementary methods

Senescence induction and SA-β-Gal assay

To induce cellular senescence, cells were seeded at 2 × 10^4/mL in plates and treated with etoposide (2 μM), GSK461364 (5 μM), irradiation (IR) (12 Gy), or IR + veliparib (12 Gy + 20 μM). For IR + veliparib, the veliparib was added 1 h prior to IR. Cells treated with DMSO vehicle or veliparib alone (20 μM) served as controls. After 5 days of culture without changing the media, cells were fixed with 2% PFA. For SA-β-Gal assay, cells were incubated for 16 to 32 h at 37 °C in staining buffer containing 1 mg/mL X-Gal (X4281C, Golden Bio), 40 mM citric acid/sodium phosphate, 150 mM NaCl, 2 mM $MgCl_2$, 3.3 mM $K_3[Fe(CN)_6]$, 3.3 mM $K_4[Fe(CN)_6]$, pH = 6. After staining, images were captured on a Zeiss Axiovert 200M microscope with a 20× Plan-NeoFluar objective and Axiocam digital camera. SA-β-Gal-positive and -negative cells were counted in more than 5 fields, yielding an average percentage indicated on each SA-β-Gal image as mean ± SD. Two or more replicates were performed.

Characterization of senescence-associated secretory phenotype (SASP)

WT or STING KO CT26 cells were treated for 4 days with DMSO control, etoposide (2 μM), GSK461364 (5 μM), IR (12 Gy), or IR + veliparib (12 Gy + 20 μM), then washed with PBS and cultured continuously for 2 days in fresh medium in order to collect conditioned media containing senescence-associated secretory phenotype (SASP) factors. The conditioned media was analyzed using the Mouse Cytokine Array C3 kit (Ray Biotech) according to the manufacturer's protocol. Briefly, the cytokine array membranes were incubated in blocking buffer for 30 min at room temperature, followed by overnight incubation in 2 mL of conditioned media at 4°C. After washing, the

membranes were sequentially incubated with Biotinylated Antibody Cocktail and HRP-Streptavidin for 2 hours at room temperature, followed by chemiluminescence detection with an iBright Imaging System (Thermo Fisher Scientific). The intensity of each cytokine-specific antibody spot was measured using Fiji and the *Protein Array Analyzer* plugin. IFN-β secretion was examined using Meso Scale Discovery (MSD) U-PLEX Mouse IFN-β Assay kit (K152G0K) according to the manufacture's protocol. Briefly, 25 µL conditioned media was added to each well of MSD plate and incubated at room temperature for 1 h with shaking. After washing, 50 µL of detection Antibody Solution was added and incubated for 1 h, followed by developing with MSD GOLD Read Buffer B using an MSD instrument.

Splenocyte cells-as-sensors assay

To obtain splenocytes, spleens were isolated from BALB/c mice bearing subcutaneous CT26 tumors, dissociated, filtered through a 40 µm cell strainer, and resuspended in basic murine immune cell culture medium. The red blood cells were lysed using Red Blood Cell Lysis Buffer (Biolegend) according to the manufacturer's protocol. CT26 SnCs were treated with IR + veliparib as described above, while proliferating CT26 cells treated with DMSO were used as controls. Both SnCs and proliferating cells were washed twice with PBS, replaced with fresh murine immune cell culture medium, then cocultured with splenocytes for 3 days. Nonadherent cells were collected and diluted to 0.5 x 10^6 cells/mL. Single cell RNA sequencing was performed using 10X Genomics Chromium technology, libraries were formed and sequenced, and data were analyzed using the Seurat package in R. Genes were considered significantly upregulated or downregulated if they displayed fold change > 1.5 and P value < 0.05, comparing coculture with SnCs or proliferating cells. The list of differentially expressed genes (DEGs) was subjected to Gene Ontology (GO) analysis by g:Profiler to detect

enriched pathways.

Phagocytosis/trogocytosis assays

Senescent and proliferating cells were prepared as described above, then labeled with PKH26 (Sigma) or pHrodo Red (IncuCyte) for 15 min at 37 °C according to the manufacturers' protocols. The cells were washed and cocultured with BMDCs in a ratio of 1:2 for 6 h. Nonadherent cells were harvested, stained with fluorophore conjugated CD11c antibody alone or in combination with CD103 antibody (BioLegend) for 45 min at 4 °C. Cells were analyzed using BD Fortessa 4-15 HTS Flow cytometer and FlowJo software. The uptake of senescent cells by BMDCs was determined using a gating strategy that allows for analysis of $CD11c^+$ or $CD11c^+/CD103^+$ single cells. Detailed information on primary antibodies is provided in Supplementary Table 1.

Analysis of BMDC maturation and STING dependence

To form a STING knockout population of CT26 cells, a set of three pre-designed sgRNAs targeting mouse *Tmem173* (*Sting1*), negative control scrambled sgRNA, and spCas9 nuclease were purchased from Synthego Corporation. For transfection, sgRNAs and spCas9 were mixed in a 3:1 ratio and incubated at room temperature for 15 min to form ribonucleoprotein (RNP) complexes, which were then delivered to CT26 cells using the Neon Electroporation System (Thermofisher Scientific) according to the manufacturer's protocol. Briefly, 2 x 10^5 CT26 cells in 10 µL Buffer R (Thermofisher Scientific) were added to 3 µL RNPs. 10 µL of the mixture was electroporated at settings of 1600 volts, 10 ms pulse length, and 3 pulses, then immediately transferred into pre-warmed cell culture medium. Cells were allowed to recover overnight. 95% editing efficiency leading to knockout was confirmed through Sanger sequencing analysis. Loss of STING protein expression was verified by Western Blot analysis. The

resulting knockout population was then used within five passages. Detailed primer information is provided in Supplementary Table 2.

To inhibit STING, CT26 or 4T1 cells were treated with senescence inducers or DMSO controls in the presence or absence of the STING inhibitor C178 (4 μM) on Day 0, then used for BMDC coculture assay on Day 5. To activate STING, we treated CT26 cells with DMSO vehicle or senescence inducers from Day 0, then added DMXAA (30 μg/mL) on Day 3 and continued culture for another 2 days. To produce damaged cells, CT26 cells were treated with 12 Gy IR or IR + veliparib (12 Gy + 20 μM), then utilized 1 day later for BMDC coculture experiments. To prepare apoptotic senescent cells, senescent CT26 cells induced by IR + veliparib were treated with ABT-263 (5 μM) overnight.

To prepare cell lysate (CL), 2.5 x 10^6 senescent cells or proliferating controls were suspended in 1 mL PBS, followed by freezing and thawing five times and centrifugation at 12,000 g/min for 10 min at 4°C. 20 or 200 μL supernatants were used for DC coculture assays. In addition, 1 mL conditioned media (CM) prepared as in SASP characterization assays was used for DC stimulation.

All tumors cells were washed twice with PBS, then cocultured with BMDCs for 12-16 h in a 1:2 ratio in basic immune cell culture medium. After coculture, nonadherent cells were collected and incubated with zombie yellow dye (BioLegend) for 10 min at room temperature, followed by staining with CD11c, CD103, CD86, CD80, PD-L1, and H-2K^d or H-2L^d MHC I antibodies for 45 min at 4°C. Cells were analyzed using a BD Fortessa 4-15 HTS Flow cytometer and FlowJo software.

Analysis of T cell cross-priming and proliferation

To prepare CT26 immunized mice, 0.5 x 10^6 CT26 or 4T1 cells were lethally irradiated (20 Gy) and then injected subcutaneously (s.q.) into 7-9 week BALB/c mice

twice over a 10-day interval. Splenocytes were isolated from immunized mice and stained with 0.5 μM carboxyfluorescein succinimidyl ester (CFSE) for 10 min at room temperature. After washing, CFSE labeled splenocytes were cocultured for 5 days in a 20:1 ratio with BMDCs pre-stimulated by senescent CT26 cells or proliferating controls. After coculture, cells were collected and incubated with zombie yellow dye (BioLegend) for 10 min at room temperature, followed by staining with CD4 and CD8a antibodies for 30 min at 4°C. Cells were analyzed using a BD Fortessa 4-15 HTS flow cytometer and FlowJo software.

Time-lapse live-cell analysis

5 x 10^4 cells per well were seeded in 6-well plates, and treated with DMSO vehicle, etoposide (2 μM), GSK461364 (5 μM), IR (12 Gy), or IR + veliparib (12 Gy + 20 μM), in the absence or presence of C178 (4 μM). The plates were then analyzed by time-lapse imaging in a IncuCyte S3 live-cell imaging system (Sartorius). Phase contrast images were acquired at 10× magnification with scanning every 2 h for 3 days. More than 16 non-overlapping fields were captured for each well. Quantitative analysis of cell confluency was performed using IncuCyte S3 2020 software.

Western blotting

To verify STING knockout (KO), 2 x 10^5 STING KO cells or Scramble controls were harvested. To examine the STING/TBK1/IRF3 signaling pathway activation, 5 x 10^4 cells were seeded per well in 6-well plates, treated with DMSO vehicle, etoposide (2 μM), GSK461364 (5 μM), IR (12 Gy), or IR + veliparib (12 Gy + 20 μM) and then harvested 5 days later. To examine the effects of DMXAA, 5 x 10^4 CT26 cells were seeded per well in 6-well plates, treated with DMAXX (30 μg/mL) and harvested 2 days later. The whole-cell lysates were prepared using RIPA lysis reagent (Thermo Fisher

Scientific) in the presence of protease and phosphatase inhibitors (Thermo Fisher Scientific). 15 µg of protein was loaded per well, separated on a NuPage 4-12% Tris-Base precast gel (Invitrogen), and transferred onto a nitrocellulose membrane (Millipore). After dividing the blots into strips, immunoblotting was performed using anti-pIRF3 (phospho-Ser396), anti-IRF3, anti-γH2AX, anti-β actin, anti-STING, anti-pTBK1 (phospho-Ser172), anti-TBK1, anti-α tubulin primary antibodies as indicated, then detected with peroxidase-conjugated secondary antibodies (Thermo Fisher Scientific, NA934vs or NA931) followed by luminescence detection using ECL substrate and an iBright Imaging System (Thermo Fisher Scientific). Detailed information on primary antibodies is provided in Supplementary Table 1.

γH2AX DNA damage foci and cytosolic DNA staining

WT or STING KO CT26 cells were seeded on sterile cover glass at $1x10^4$ per well in 24-well plates. Cells were treated for 5 days with DMSO control, veliparib alone (20 µM), IR (12 Gy), or IR + veliparib (12 Gy + 20 µM), etoposide (2 µM), or GSK461364 (5 µM), and then fixed with 4% PFA for 10 min at room temperature. For γH2AX foci staining, cells were permeabilized with 0.2% Triton-X for 10 min. After blocking with 5% BSA-PBS, cell slides were incubated overnight at 4°C with primary antibody against γH2AX (Millipore, 05-636, 1:1000) diluted in 5% BSA. For cytosolic DNA staining, 5% BSA-PBS supplemented with 0.1% Saponin was used for blocking and antibody dilution. Cell samples were blocked for 1 h at room temperature, followed by overnight incubation with primary antibody against dsDNA (Santa Crutz, HYB331-01, 1:100) at 4°C. Following PBS washes, DAPI (1 mg/mL) and fluorescent secondary antibodies (Jackson ImmunoResearch, 1:2000,) diluted in 5% BSA-PBS ± 0.1% Saponin were applied for 1 h at room temperature. Cell slides were mounted with ProLong Gold Antifade Mountant (Thermo Fisher Scientific) after PBS washes. Images

were captured on a Zeiss Axiovert 40CFL with a 40X Plan-NeoFluar objective and pseudo-colored using Fiji. Three replicates were performed. Detailed information on primary antibodies is provided in Supplementary Table 1.

Flow cytometric analysis of AH-1 specific T cells

7-8 week BALB/c mice received subcutaneous (s.q.) injection of 0.5 x 10^6 CT26 SnCs or PBS control. 2 days later, the draining inguinal lymph nodes were isolated, dissociated and stained with FITC AH-1 dextramer (Immudex) according to manufacturer's protocol. Briefly, ~ 2 x 10^6 cells in 50 µL staining buffer were incubated with AH-1 dextramer for 10 min at room temperature, then Alexa Fluor 647 CD8 antibody (Clone KT15, BioRad) was added for another 20 min in the dark. After washing, cells were analyzed using BD Fortessa 4-15 HTS flow cytometer and FlowJo software.

Preventative and therapeutic vaccination with SnCs or SnC-activated DCs

For preventative vaccination, 7-8 week BALB/c or NSG mice received subcutaneous (s.q.) injection of 0.5 x 10^6 CT26 SnCs in 100 µL PBS or PBS alone on Day -5, and/or intravenous (i.v.) injection of α-PD-L1 antibody (BioXCell, 0.2 mg in 100 µL PBS) on Day -4. The naive or vaccinated mice were challenged by s.q. injection of 0.5 x 10^6 CT26 or 4T1 cells in 100 µL PBS on Day 0. Tumor growth was monitored every 2-3 days for 4 weeks and the tumor volume was measured using a caliper from day 7 after tumor inoculation.

For therapeutic vaccination, 7-8 week BALB/c mice were inoculated s.q. with 0.25 or 0.5 x 10^6 CT26 or 4T1 cells in 100 µL PBS on Day 0. To initiate treatment, 0.5 x 10^6 SnCs or SnC-activated DCs in 100 µL PBS were injected peritumorally on Days 9 or 12, at tumor volumes of ~ 60 mm^3 or 150 mm^3, and then again on Days 14 or 19,

respectively. Where indicated, on Days 12 or 15, mice also received a single i.v. injection of α-PD-L1 antibody (0.2 mg) or a single 10 Gy radiation delivered using a RadSource RS-2000 X-Ray generator operating at 160 kV and 25 mA, calibrated by NIST traceable dosimetry. Tumor volume was measured using calipers every 2-3 days from day 7 after tumor inoculation.

In tumor re-challenge experiments, naive controls or mice whose tumors were eradicated by treatment with SnC-activated DC vaccine and irradiation and that remained tumor free for >10 days were injected s.q. with 0.5 x 10^6 CT26 cells on the back. Tumor growth was monitored every 2-3 days for 3 weeks.

Flow cytometric analysis of tumor infiltrating immune cells

CT26 or 4T1 tumors were collected 5 days after their last treatment and divided in half for either flow cytometric or histological analyses. For flow cytometry, the tumors were dissociated using a Miltenyi Tumor Dissociation Kit. Briefly, tumor tissues were transferred into the gentleMACS C Tubes containing enzyme mix. Then the C tubes were run on a gentleMACS Dissociator using gentleMACS program m_impTumor_02. After termination of the program, samples were incubated for 30 min at 37 °C. After dissociation, the cell suspensions were filtered through a 70 μm cell strainer and pelleted by centrifugation at 300 × g for 5 min. The cell pellet was resuspended in PBS, incubated with zombie yellow dye (BioLegend) for 10 min at room temperature, washed, and stained with fluorophore conjugated CD45, CD3, CD4, CD8, CD49b, CD11c, and CD103 antibodies for 30 min at 4°C, followed by analysis using a BD Fortessa 4-15 HTS flow cytometer and FlowJo software. Detailed information on primary antibodies is provided in Supplementary Table 1.

Lung colonization assays

7-8 week female BALB/c mice were inoculated intravenously (i.v.) with 6 x 10^4 or 8 x 10^4 proliferating 4T1 cells on Day 0, delivering disseminated tumor cells to the lungs. For preventative vaccination, 0.5 x 10^6 4T1 SnCs in 100 µL PBS were injected subcutaneously (s.q.) on Days -5 and -1. For therapeutic vaccination, 0.5 x 10^6 4T1 SnCs or 0.5 x 10^6 4T1 SnC-activated DCs in 100 µL PBS were injected s.q. on Days 1 and 5. Where indicated, mice also received a single i.v. dose of α-PD-L1 antibody (0.2 mg) on Day 3. On Day 21, mice were euthanized, lungs were perfused with 1 mM EDTA-PBS, fixed with 10% neutral formalin, and then examined visually for surface metastatic foci and/or embedded and sectioned for histological analysis to evaluate colonization in lung parenchyma.

Histology and immunofluorescence

The remaining halves of the CT26 or 4T1 tumors were fixed with 10% neutral formalin for histological analysis. Alternatively, mouse lungs were collected, perfused with 1 mM EDTA-PBS and fixed with 10% neutral formalin. Tissue processing, embedding, and sectioning were performed by the Human Tissue Resource Center at the University of Chicago. 5 µm sections were stained with hematoxylin and eosin (H&E) and scanned using a CRi Pannoramic SCAN 40x Whole Slide Scanner. For immunofluorescence, tumor sections were deparaffinized with xylene, rehydrated, and immersed in 10 mM sodium citrate buffer (pH 6.0) for 30 min at 90 °C for antigen retrieval. After blocking with 5% BSA, the samples were stained with CD8, perforin, and granzyme B primary antibodies at 4 °C overnight, washed, then stained with fluorophore-conjugated secondary antibodies (Vector Labs), counterstained with DAPI, mounted and scanned using an Olympus VS200 SlideView Whole Slide Scanner.

Supplementary figure legends

Supplementary Figure 1

SnCs primarily affect conventional type 1 dendritic cells

A, SA-β-Gal staining of CT26 cells. CT26 cells were treated with DMSO vehicle or IR + veliparib (12 Gy + 20 μM), followed by fixation and staining 5 days later. The mean ± SD percentage of SA-β-Gal-positive SnCs in five 20× fields is indicated. Scale bars: 200 μm. **B**, Experimental schema for scRNA-seq analysis of splenocytes after coculturing with CT26 proliferating controls or SnCs prepared as in **A** with 12 Gy + veliparib. **C,** tSNE analysis of scRNA-seq of nonadherent cells after splenocytes were cocultured with proliferating controls (cyan, n=593) or SnCs (red, n=1024) for 3 days. **D**, Stacked bar graph showing the relative proportion of 11 cell clusters after coculturing with proliferating cells or SnCs. cDC2, conventional type 2 dendritic cell. HSC, hematopoietic stem cell. APC, antigen-presenting cell. **E**, Scatter plots from scRNA-seq clusters showing the differential gene expression (DGE) in splenocytes cocultured with proliferating controls or SnCs. Dots indicate relative expression in each cluster for a single detected gene. Blue lines indicate equal expression and R^2, the goodness of fit. All genes that passed quality control were analyzed. cDC1, conventional type 1 dendritic cell. cDC2, conventional type 2 dendritic cell. **F**, Reactome Gene Ontology (GO) analysis and **G**, Kyoto Encyclopedia of Genes and Genomes (KEGG) enrichment analysis of upregulated differentially expressed genes (DEGs) in cDC1 after coculturing with SnCs confirm Biological Process-enriched pathways. Dots indicate the number of DEGs and bars the -Log10 (p-value) for each enriched pathway.

Supplementary Figure 2

Senescent cells secrete more cytokines compared to proliferating cells

A, Cytokine array analysis of the conditioned media. CT26 cells were treated for 4 days with DMSO vehicle, etoposide (2 μM), GSK461364 (5 μM), IR alone (12 Gy), or IR + veliparib (12 Gy + 20 μM), washed, then continuously cultured in fresh medium for 2 days to collect the conditioned media. Color-coded rectangle frames indicate the position of SASP factors that have dramatically changed in senescent cells compared to proliferating cells. **B**, Complete list of cytokines detected by the array.

Supplementary Figure 3

Gating strategy of flow cytometric analysis

A, To examine the effects of coculture, cells were first gated based on forward scatter (FSC-A and FSC-H) for the single cell population. Then $CD11c^+$ DCs were selected for quantification analysis of PKH26 intensity. **B**, Cells were first gated for single live cells by size and Zombie yellow exclusion, then gated on co-expression of CD11c and CD103 to identify DCs. The DC population was analyzed for pHrodo Red intensity. **C**, DCs were identified as in **B**, and then analyzed for surface expression of activation/maturation markers CD80, CD86, $H\text{-}2K^d$, and PD-L1. **D**, To evaluate T cell proliferation, cells were gated on size and viability and then further gated into $CD8^+$ and $CD4^+$ T cell populations. CFSE dilution was measured in both $CD8^+$ and $CD4^+$ T cells. **E**, To examine the effects of ABT263, CT26 SnC single-cell population was selected based on forward scatter (FSC-A and FSC-H), and apoptosis was analyzed by Annexin V binding and propidium iodide (PI) uptake. **F**, To examine CT26-reactive CTLs, cells gated on size and $CD8^+$ expression were analyzed for AH-1 dextramer binding. **G**, Dissociated tumor cells gated on size, viability, and CD45 were evaluated for NK cells ($CD49b^+/CD3^-$) and T cells ($CD3^+/CD49b^-$), which were further gated into $CD8^+$ and

CD4$^+$ T cell populations. **H**, Live CD45$^+$ immune cells were gated as in **G,** followed by the identification of dendritic cells (DCs, CD11c$^+$/CD103$^+$).

Supplementary Figure 4

SnCs are effectively engulfed by BMDCs *in vitro*

To evaluate uptake of SnCs by BMDCs, CT26 (**A**) or 4T1 (**B**) SnCs were induced by IR (12 Gy), IR + veliparib (12 Gy + 20 μM), or etoposide (2 μM). Proliferating CT26 and 4T1 cells were used as controls. BMDCs were cocultured with pHrodo Red-labeled cells for 6 h, followed by staining and flow cytometric analysis. The geometric mean fluorescence intensity (MFI) of pHrodo Red was determined in the single, viable, CD11c$^+$/CD103$^+$ cell population. Data from three experiments, mean ± SD. *** $P < 0.001$, ** $0.001 < P < 0.01$, * $0.01 < P < 0.05$ (paired t-test).

Supplementary Figure 5

Senescent 4T1 cells promote DC maturation/activation and T cell priming *in vitro*

A, SA-β-Gal staining of 4T1 cells. 4T1 cells treated with DMSO vehicle or veliparib (20 μM) were used as controls. Cellular senescence was induced by IR (12 Gy), IR + veliparib (12 Gy + 20 μM), etoposide (2 μM), or GSK461364 (5 μM). The mean ± SD percentage of SA-β-Gal-positive cells from five 20× fields is indicated. Scale bars: 200 μm. **B**, Phagocytosis assays indicating effective uptake of senescent cells (SnCs) by BMDCs. 4T1 SnCs and controls were prepared as in **A**. BMDCs were cocultured with PHK26 labeled 4T1 cells for 6 h, followed by staining and flow cytometric analysis to determine PHK26 MFI in the CD11c$^+$ DC population. Data from three experiments, mean ± SD. **C**, For quantitative analysis of DC activation/maturation, BMDCs were cocultured overnight with 4T1 SnCs and controls as prepared in **A**, stained for CD80, CD86, H-2K^d, and PD-L1, and analyzed by flow cytometry to determine MFI in single,

viable, $CD11c^+/CD103^+$ DCs. Data from three experiments, mean ± SD. For statistical analysis, *** $P < 0.001$, ** $0.001 < P < 0.01$, * $0.01 < P < 0.05$ (paired t-test). **D** and **E**, T cell priming by SnC-activated DCs. CFSE-labeled splenocytes were cocultured for 5 days with DCs stimulated by 4T1 SnCs or controls as in **C,** in the absence or presence of α-PD-L1. Shown are the % proliferative (CFSE diluted) fraction of viable $CD8^+/CD4^-$ (**D**) or $CD8^-/CD4^+$ (**E**) T cells.

Supplementary Figure 6

T cell priming by CT26 SnC-loaded DCs

Primary flow cytometry data linked to **Fig. 2F** and **G**. CFSE-labeled splenocytes cocultured for 5 days with DCs pre-stimulated by CT26 proliferating or senescent cells in the absence (**A** and **C**) or presence (**B** and **D**) of α-PD-L1. Shown are zombie $yellow^-/CD8^+/CD4^-$ (**A** and **B**) and zombie $yellow^-/CD4^+/CD8^-$ (**C** and **D)** T cell populations, indicating % proliferating cells.

Supplementary Figure 7

T cell priming by 4T1 SnC-loaded DCs

Primary flow cytometry data linked to **Fig. S3E** and **F.** CFSE-labeled splenocytes cocultured for 5 days with DCs pre-stimulated by proliferating or senescent 4T1 cells in the absence (**A** and **C**) or presence (**B** and **D**) of α-PD-L1. Shown are zombie $yellow^-/CD8^+/CD4^-$ (**A** and **B**) and zombie $yellow^-/CD4^+/CD8^-$ (**C** and **D)** T cell populations, indicating % proliferating cells.

Supplementary Figure 8

DC stimulation by SnC lysates and conditioned media and increased cytoplasmic DNA, STING activation, and IFN-β secretion in SnCs

A, BMDCs were cocultured overnight with cells, cell lysates (CL) or conditioned media (CM) derived from proliferating controls or senescent cells. Surface expression of CD80, CD86, H-2K^{d}, and PD-L1 was analyzed by flow cytometry to determine MFI in single viable CD11c^{+}/CD103^{+} DCs. Data from three experiments, mean ± SD. **B** and **C,** Representative pseudo-colored images of staining for DNA damage marker γH2AX (red) (**B**) or cytoplasmic DNA (red) (**C**), overlaid with DAPI (blue). Cell contours on bright-field images are indicated by yellow dotted lines (**C**). CT26 cells were treated for 5 days with DMSO vehicle, veliparib alone (20 μM), IR (12 Gy), IR + veliparib (12 Gy + 20 μM), etoposide (2 μM), or GSK461364 (5 μM). Scale bars: 20 μm. **D**, Western blot analysis indicates the upregulation of γH2AX and IRF3 phosphorylation in senescent cells. Cells were treated as in **B**. Shown are representative Western blot results for γH2AX (phospho-Ser139), p-IRF3 (phospho-Ser396), total IRF-3, and β-tubulin loading control of whole-cell lysates, loaded with 15 μg protein per lane. **E**, Meso Scale Discovery (MSD) Immunoassay analysis of IFN-β secretion in the conditioned media. CT26 cells were treated as in **B** for 4 days, then washed and cultured in fresh medium for another 2 days to collect the conditioned media. Data from four experiments, mean ± SD. For statistical analysis, *** $P < 0.001$, ** $0.001 < P < 0.01$ (paired t-test).

Supplementary Figure 9

STING is not required for senescence induction in CT26 cells

A, Western blot verification of STING knockout (KO) in CT26 cells. CT26 cells were electroporated with RNPs formed with gRNAs targeting *Teme173* (*Sting1*) or scramble gRNA control. Shown are representative Western blot results of whole-cell lysates from passage 5 after transfection. **B** and **C**, Automated cell growth analysis from time-lapse imaging over 3 days. Scramble (Scr, **B**) and STING KO CT26 cells (**C**) were treated with DMSO, IR (12 Gy), IR + veliparib (12 Gy + 20 μM), etoposide (2 μM), or

GSK461364 (5 μM) at time 0. Results are shown as mean ± SEM. Images of 16 non-overlapping fields were captured for analysis of each sample. **D**, SA-β-Gal staining of CT26 cells. Scr or STING KO CT26 cells were treated as in **B** and **C**, followed by fixation and staining after 5 days. The mean ± SD percentage of SA-β-Gal-positive cells from five 20× fields is indicated. Scale bars: 200 μm. **E** and **F**, Representative pseudo-colored images of staining for DNA damage marker γH2AX (red) (**E**) or cytoplasmic DNA (red) (**F**), overlaid with DAPI (blue). Cell contours on bright-field images are indicated by yellow dotted lines (**F**). Scr or STING KO CT26 cells were treated as in **D**. Scale bars: 20 μm.

Supplementary Figure 10

STING signals modulate the expression of CCL5 and MHC class I molecules in senescent CT26 cells

A, Cytokine array analysis of the conditioned media. STING KO CT26 cells were treated with DMSO vehicle, etoposide (2 μM), or IR + veliparib (12 Gy + 20 μM) for 4 days, then washed and cultured in fresh medium for another 2 days to collect the conditioned media. Color-coded rectangle frames indicate the position of SASP factors that have dramatically changed in senescent cells compared to proliferating cells. **B**, Quantitative analysis of cytokine secretion by non-senescent or senescent Scramble or STING KO CT26 cells. **C**, Quantitative analysis of MHC I molecules expression. Scramble or STING KO CT26 cells were treated for 5 days with DMSO, IR (12 Gy), IR + veliparib (12 Gy + 20 μM), etoposide (2 μM), or GSK461364 (5 μM), then stained for H-2K^d, H-2D^d, or H-2L^d and analyzed by flow cytometry to determine MFI in single cell population. Data from three experiments, mean ± SD. *** $P < 0.001$, ** $0.001 < P < 0.01$, n.s. $P > 0.05$ (paired t-test).

Supplementary Figure 11

STING is required for CT26 SnCs to activate DCs

A, Automated cell growth analysis from time-lapse imaging. CT26 cells were treated with DMSO, IR (12 Gy), IR + veliparib (12 Gy + 20 μM), etoposide (2 μM), or GSK461364 (5 μM) in the absence or presence of C178 (4 μM) at time 0. Images were captured over 3 days for each condition at a 2-hour interval. Results are shown as a fit to the mean ± SEM of 16 non-overlapping fields for each sample at each time point. **B,** SA-β-Gal staining of CT26 cells. Cells were treated as in **A**, followed by fixation and staining after 5 days. The mean ± SD percentage of SA-β-Gal-positive cells from five 20× fields is indicated. Scale bars: 200 μm. **C**, Quantitative analysis of DC activation/maturation. BMDCs were cocultured overnight with CT26 cells treated as in **A.** The single viable $CD11c^+/CD103^+$ DC population was analyzed for MFI of CD80, CD86, H-$2K^d$, and PD-L1. Data from three experiments, mean ± SD. *** $P < 0.001$, ** $0.001 < P < 0.01$, n.s. $P > 0.05$ (paired t-test).

Supplementary Figure 12

STING is required for 4T1 SnCs to activate DCs

A, Automated time-lapse imaging analysis of growth kinetics of 4T1 cells treated at time 0 with DMSO, IR (12 Gy), IR + veliparib (12 Gy + 20 μM), etoposide (2 μM), or GSK461364 (5 μM) in the absence (left) or presence (right) of C178 (4 μM). Shown is the non-linear fit to the mean ± SEM of 16 non-overlapping fields for each sample at indicated time point. **B**, SA-β-Gal staining of 4T1 cells. Cells were treated as in **A**, followed by fixation and staining after 5 days. The mean ± SD percentage of SA-β-Gal-positive cells from five 20× fields is indicated. Scale bars: 200 μm. **C**, Quantitative analysis of DC activation/maturation. BMDCs were cocultured overnight with 4T1 cells treated as in **A.** The single viable $CD11c^+/CD103^+$ DC population was analyzed for MFI

of CD80, CD86, H-2K^d, and PD-L1. Data from three experiments, mean ± SD. *** P < 0.001, ** 0.001 < P < 0.01, n.s. P > 0.05 (paired t-test).

Supplementary Figure 13

STING/TBK1/IRF3 signaling activation in tumor cells is not sufficient for DC activation but is necessary for senescent cells to serve as protective vaccines

A, The STING agonist DMXAA (30 μg/mL) activates STING signals in CT26 cells after two days of treatment. Shown are representative Western blot results for p-TBK1 (phospho-Ser172), total TBK1, and β-actin loading control of whole-cell lysates, loaded with 15 μg protein per lane. **B**, Quantitative analysis of DC activation/maturation. Cellular senescence was induced using etoposide (2 μM) or IR + veliparib (12 Gy + 20 μM). The non-senescent or senescent Scramble or STING KO CT26 cells were pretreated for 2 days with or without DMXAA (30 μg/mL), washed, and then cocultured overnight with BMDCs. The Zombie yellow-/CD11c+/CD103+ DC population was analyzed for MFI of CD80, CD86, H-2K^d, and PD-L1. Data from three experiments, mean ± SD. *** P < 0.001, ** 0.001 < P < 0.01, * 0.01 < P < 0.05, n.s. P > 0.05 (paired t-test). **C**, BALB/c mice injected with 0.5 x 10^6 Scramble (Scr) or STING KO CT26 SnCs at Day -5 were challenged with 0.5 x 10^6 CT26 proliferating cells on Day 0 and examined for palpable tumors at 2-3 day intervals (n = 7 per group). Shown is Kaplan-Meier analysis of CT26 tumor incidence over time. 6/7 Scr SnC-vaccinated mice and 2/7 STING KO-vaccinated mice did not develop tumors. Logrank test. *** P < 0.001, * 0.01 < P < 0.05.

Supplementary Figure 14

CT26 SnC vaccines suppress tumor growth and potentiate cancer therapies

Individual tumor growth data linked to **Fig. 5A-F. A,** Experimental schema for treating CT26 tumor bearing mice with SnC vaccine and/or α-PD-L1, initiating treatment at Day 9. **B-E**, Growth kinetics of individual CT26 tumors untreated (**B**), treated with SnC vaccine (**C**), α-PD-L1 (**D**), or the combination therapy (**E**). **F**, Experimental schema for treating CT26 tumor bearing mice with SnC vaccine and/or 10 Gy irradiation (IR). **G-J**, Growth kinetics of individual CT26 tumors untreated (**G**), treated with SnC vaccine (**H**), IR (**I**), or the combination therapy (**J**).

Supplementary Figure 15

CT26 SnC vaccines suppress tumor growth and potentiate cancer therapies

A, Experimental schema for treating CT26 tumor bearing mice with SnC vaccine and/or α-PD-L1, initiating treatment at Day 12. **B,** Growth kinetics of CT26 tumors untreated, treated with SnC vaccine, α-PD-L1, or combination therapy (n = 5-7 per group, mean ± SEM). **C**, CT26 tumor weight at Day 30. Shown are individual tumor weights (circle) and weight range (box and whisker). **D-G**, Individual tumor growth data linked to **B.** Shown are growth kinetics of individual CT26 tumors untreated (**D**), treated with SnC vaccine (**E**), α-PD-L1 (**F**), or the combination therapy (**G**). **H**, Experimental schema for treating CT26 tumor bearing mice with SnC vaccine and/or 10 Gy irradiation (IR), initiating treatment at Day 12. **I**, Growth kinetics of CT26 tumors untreated, treated with SnC vaccine, IR, or combination therapy (n = 5-7 per group, mean ± SEM). **J**, CT26 tumor weight at Day 30. Shown are individual tumor weights (circle) and weight range (box and whisker). **K-N**, Individual tumor growth data linked to **I.** Shown are growth kinetics of individual CT26 tumors untreated (**K**), treated with SnC vaccine (**L**), IR (**M**), or combination therapy (**N**). For statistical analysis, *** $P < 0.001$, ** $0.001 < P < 0.01$, * $0.01 < P < 0.05$, n.s. $P > 0.05$ (paired t-test).

Supplementary Figure 16

Senescent 4T1 cell vaccines suppress tumor growth and potentiate immunotherapy

A, Experimental schema for treating 4T1 tumor-bearing mice with SnC vaccine and/or α-PD-L1. **B,** Growth kinetics of 4T1 tumors untreated, treated with SnC vaccine, α-PD-L1, or the combination therapy (n = 5-7 per group, mean ± SEM). **C**, 4T1 tumor size at Day 30. Shown are individual tumor sizes (circle) and size range (box and whisker). *** $P < 0.001$, ** $0.001 < P < 0.01$, * $0.01 < P < 0.05$, n.s. $P > 0.05$ (paired t-test). **D-G**, Individual tumor growth data linked to **B.** Growth kinetics of individual 4T1 tumors untreated (**D**), treated with SnC vaccine (**E**), α-PD-L1 (**F**), or combination therapy (**G**).

Supplementary Figure 17

CT26 SnC vaccine promotes CTL infiltration and activation

A, Representative H&E staining of CT26 tumor sections. CT26 tumors excised at Day 18 (5 days after second SnC injection) were divided, fixed, embedded and sectioned. Serial sections as in **Fig. 5H** were used. Shown are representative whole section scanning (upper panel, scale bar: 2 mm) and selected enlarged regions (lower panel, scale bar: 200 μm). **B**, Immunofluorescence staining of serial sections to H&E in **A** for activated CTL infiltrate with markers CD8 (red), granzyme B (green), and DAPI (blue). Scale bars: 200 μm.

Supplementary Figure 18

4T1 SnC vaccine promotes CTL infiltration and activation

A, Analysis of immune infiltrate in 4T1 tumors. Mice bearing subcutaneous 4T1 tumors were untreated or treated with SnC vaccine, α-PD-L1, or combination therapy as in **Fig. S2**. Tumors excised at Day 18 (5 days after second SnC injection) were divided,

dissociated and stained for flow cytometry. The viable, single cell population was analyzed for total immune ($CD45^+$), DC ($CD11c^+/CD103^+$), T_h ($CD3^+/CD4^+/CD8^-$), CTL ($CD3^+/CD8^+/CD4^-$), and NK ($CD3^-/CD49b^+$) cells. Shown are individual tumors (open circles, n = 3 per group) and mean ± SD (bar). *** P < 0.001, ** 0.001 < P < 0.01, * P < 0.05, n.s. P > 0.05 (paired t-test). **B**, The remaining portion of the 4T1 tumors examined in **A** were fixed, embedded and sectioned. Shown are representative H&E whole section scanning (scale bar: 2 mm) and selected enlarged regions (scale bar: 200 μm). **C** and **D**, Immunofluorescence staining of serial sections to the H&E in **B** for activated CTL infiltrate with (**C**) markers CD8 (yellow), perforin (red), and DAPI (blue), or (**D**) CD8 (red), granzyme B (green), and DAPI (blue). Scale bars: 200 μm.

Supplementary Figure 19

4T1 SnC vaccines suppress lung colonization

A, Experimental schema for treating with SnC vaccines to limit lung colonization. BALB/c mice were injected i.v. with 8 x 10^4 4T1 proliferating cells on Day 0 and then treated with 0.5 x 10^6 4T1 SnCs on Days -5 and -1 or Days 1 and 5 as preventative or therapeutic vaccines, respectively. Lungs were collected on Day 21. **B**, Quantification of metastatic foci on lung surface. Shown are counts from individual lungs (dot), with mean ± SEM (bar). ** 0.001 < P < 0.01, * P < 0.05 (paired t-test). **C**, Representative H&E staining of colonization at low magnification with inset zoomed to high magnification. Scale bars: 2 mm (upper) and 50 μm (lower).

Supplementary Figure 20

SnC-activated DC vaccine potentiates radiotherapy

Individual tumor growth data linked to **Fig. 7A-C. A,** Experimental schema for treating CT26 tumor bearing mice with SnC-activated DC vaccine and/or IR. **B-E**, Growth

kinetics of individual CT26 tumors untreated (**B**), treated with SnC-activated DC vaccine (**C**), IR (**D**), or combination therapy (**E**).

Supplementary Table 1
List of antibodies used

Antibody	Company	Catalog #	Dilution
Flow Cytometry			
Pacific Blue™ anti-mouse CD11c	BioLegend	117321	1:100
Brilliant Violet 711 anti-mouse CD103	BioLegend	121435	1:100
PE/Cyanine7 anti-mouse CD86	BioLegend	105013	1:100
APC anti-mouse CD8a	BioLegend	100711	1:100
CD274 (PD-L1, B7-H1) antibody	Invitrogen	12-5982-81	1:100
Alexa Fluor 488 anti-mouse H-2K^{d}	BioLegend	116609	1:100
PE anti-mouse H-2L^{d}/H-2D^{b}	BioLegend	114507	1:100
PE anti-mouse H-2D^{d} Antibody	BioLegend	110607	1:100
Alexa Fluor 700 anti-mouse CD45	BD Bioscience	560510	1:100
Pacific Blue™ anti-mouse CD3	BioLegend	100213	1:100
APC anti-mouse CD49b	BioLegend	108909	1:100
PE/Cyanine7 anti-mouse CD4	BioLegend	100421	1:100
BB515 anti-mouse CD8a	BD Bioscience	564422	1:100
Alexa Fluor 647 anti-mouse CD8α	BioRad	MCA609	1:100
Immunofluorescence			
CD8	Invitrogen	MA1-10301	1:500
Perforin	Cell Signaling Technology	44865	1:500
Granzyme B	Cell Signaling Technology	44153	1:500
Anti-phospho-Histone H2A.X (Ser139) Antibody, clone JBW301	Millipore Sigma	05-636	1:1000
ds DNA Marker Antibody (HYB331-01)	Santa Cruz	sc-58749	1:200
Western Blot			
Phospho-IRF3 (Ser379)	Cell Signaling Technology	4947	1:1000
IRF-3 (D83B9)	Cell Signaling Technology	4302	1:1000
Phospho-Histone H2A.X (Ser139)	Cell Signaling Technology	9718	1:1000
STING	Cell Signaling Technology	13647	1:1000
Phospho-TBK1 (Ser172)	Cell Signaling Technology	5483	1:1000
TBK1/NAK (E8I3G)	Cell Signaling Technology	38066	1:1000
β-actin (HRP conjugate)	Proteintech	HRP-60008	1:5000
α-tubulin (HRP conjugate)	Proteintech	HRP-60031	1:5000

Supplementary Table 2
Sequences of oligonucleotides used

sgRNA targeting *Tmem173*	GCGAGGCUAGGUGAAGUGCU
sgRNA targeting *Tmem173*	GAUGAUCCUUUGGGUGGCAA
sgRNA targeting *Tmem173*	ACCUGCAUCCAGCCAUCCCA
Forward primer for PCR	AGGGAAGGCCAAGGTTAGGA
Reverse primer for PCR	GGCGTCTCCTTGAGGTGTAT
Sequence primer for Sanger Sequencing	GTCTCCTTGAGGTGTATCCAAGAGTAGC